

# **XV Conference of Young Scientists "Problems of Theoretical Physics"**

Tuesday 10 June 2025 - Thursday 12 June 2025

BITP & Zoom

## **Book of Abstracts**



# Contents

Physical systems in a noncommutative space with preserved time-reversal and rotational symmetries 1

Studying the Entanglement of Multiqubit States with Quantum Technologies . . . . . 1

Meta-fibers: merging nanophotonics and fibers . . . . . 2

Engineering of plasmonic anisotropic nanopatch-based metasurfaces . . . . . 3

Enhancement of chiral sensing with plasmonics meta-gratings . . . . . 3

Spin-directional coupling in hyperbolic shear metasurfaces . . . . . 4

STRUCTURE OF HYPERNUCLEUS  ${}^7_{\Lambda}\text{Li}$  WITHIN THE THREE-CLUSTER MODEL . . . . . 5

ON INTERACTION OF LAMBDA HYPERON WITH LIGHTEST NUCLEI IN TWO-CLUSTER MODEL . . . . . 6

Loop Divergences in the Effective Theory of Chern–Simons Boson–Fermion Couplings . 7

Induced Vacuum Magnetic Flux in the Background of a Linear Topological Defect. The case of fermion matter . . . . . 9

Integrated HydroKinetic Model at Relativistic Heavy Ion Collider Energies . . . . . 10

A question concerning phase transitions in a pion system of particles and antiparticles . 11

Systematic Investigation of Density Fluctuations in Laser Wakefield Accelerators on the Properties of the Accelerated Electrons . . . . . 11

High-order cumulants near the critical point from molecular dynamics . . . . . 11

Femtoscscopy of rotating sources . . . . . 12

Search for hidden particles in intensity frontier experiments . . . . . 12

Longitudinal Josephson effect in bilayer systems with electron-hole pairing . . . . . 13

Viscoelastic response and anisotropic hydrodynamics in Weyl semimetals . . . . . 13

TUNNEL MAGNON TRANSFER THROUGH A FERROMAGNETIC CHAIN . . . . . 14

Manipulating domain wall mobility by cross section tailoring in ferromagnetic nanostripes . . . . . 14

MODELING OF THREE-COMPONENT MULTI-PARTICLE DISCRETE CONGLOMERATIONS . . . . .	15
Graphene phonons revisited . . . . .	16
Detection and identification of impurity components by THz scattering . . . . .	17
Chosen topics in topological condensed matter . . . . .	18
Partition Function Zeros and Finite-Size Effects in the Blume–Capel Model on a Complete Graph . . . . .	18
Effective form factors for asymptotics of finite-temperature correlation functions . . . .	18
Zeros of isomonodromic tau functions and holomorphic anomaly equation . . . . .	19
Integrable spinning fluid . . . . .	19
Perturbative connection formulas for Heun equations . . . . .	20
Motion in perturbed Schwarzschild space-time . . . . .	20
Defect fusion in higher dimensions . . . . .	20
Isomonodromic tau function for Painleve I equation via irregular conformal blocks of rank $5/2$ . . . . .	21
$1/2$ -BPS line defects in 4d $N=2$ SQFTs via Cohomological Hall algebras . . . . .	21
Statistical model of dimers and counting of boxes . . . . .	22
Angular Power Spectrum of the 21 cm Signal from the Dark Ages: Sensitivity to Cosmo- logical Parameters . . . . .	22
Sensitivity of the redshifted 21 cm signal from Dark Ages to parameters of primordial mag- netic fields . . . . .	23
Bayesian analysis of Starobinsky and Higgs inflation models with reheating in light of ACT and DESI data releases . . . . .	23
An Axion Pulsarscope . . . . .	24
Dynamical Friction for Plummer Sphere in Ultralight Dark Matter . . . . .	24
Hydrodynamical Modeling of Stellar Wind Bubbles for Improved Photoionization Analysis . . . . .	25
Detailed Photoionization Analysis of Chemodynamical Simulation Results for the Evolu- tion of Dwarf Star-Forming Galaxies at an Age of 100 Myr . . . . .	25
Multicomponent Photoionization Modelling of the First Dwarf Galaxies . . . . .	26
Photoionization analysis of chemodynamical simulations: Cloudy C23.01 vs C08.00 . . .	27
The interaction between physics and machine learning: attractive or repulsive? . . . .	28
A neural network model of the dependence of the energy of biomolecules on structure and quantum-mechanical descriptors . . . . .	28

Galaxy Morphological Classification with Manifold Learning . . . . .	29
Accelerating Relativistic Heavy-Ion Collision Modeling: Machine Learning Integration with the iHKM Framework . . . . .	29
Implementation of a methodology for crystal structure prediction using genetic algorithms integrated into the Python ASE library . . . . .	30
Predicting superconductors critical temperature via machine leaning methods . . . . .	30
Broadband single-layer dielectric anti-reflective solar cell coatings . . . . .	31



## Quantum Technologies, Foundations and Optics

### Physical systems in a noncommutative space with preserved time-reversal and rotational symmetries

**Author:** Prof. Khrystyna Gnatenko<sup>1</sup>

<sup>1</sup> *Ivan Franko National University of Lviv*

**Corresponding Author:** khrystyna.gnatenko@gmail.com

Physical systems in a noncommutative space with preserved time-reversal and rotational symmetries

We consider a space with noncommutativity of coordinates and momenta with preserved time-reversal and rotational symmetries [1]. The noncommutative algebra is constructed by generalizing the parameters of coordinate and momentum noncommutativity to tensors, defined with the help of additional coordinates and momenta. They are governed by a rotationally invariant system. The resulting algebra is equivalent to a canonical-type noncommutative algebra and does not violate rotational or time-reversal symmetries [1].

We examine one- and many-particle systems in this space, including free particles, systems of harmonic oscillators, and exotic atoms. We derive corrections to the energy levels of these systems caused by space quantization [2]. Additionally, we discuss the problem of describing the motion of a macroscopic body in such a space. We propose conditions on the parameters of the noncommutative algebra that provide a resolution to the soccer-ball problem in noncommutative space.

Motion of a particle and a macroscopic body in gravitational field is examined in the noncommutative phase space. The problem of the violation of the weak equivalence principle is discussed [3,4]. On the basis of comparison of the results of theoretical studies with the experimental ones the upper bound on the minimal length and the minimal momentum are found [1].

1. Kh. P. Gnatenko, Minimal momentum estimation in noncommutative phase space of canonical type with preserved rotational and time reversal symmetries, *Eur. Phys. J. Plus* 135(8), 652 (2020).
2. Kh. P. Gnatenko, System of interacting harmonic oscillators in rotationally invariant noncommutative phase space, *Phys. Lett. A* 382(46), 3317 (2018).
3. Kh. P. Gnatenko, M. I. Samar, V. M. Tkachuk, *Kepler Problem in Quantized Space*. Lviv: Lviv University Press, 2024. 136 pages.
4. Kh. P. Gnatenko, V. M. Tkachuk, Deformed Heisenberg algebras of different types with preserved weak equivalence principle, *J. Phys. Stud.* 27(1), 1001 (2023).

### Studying the Entanglement of Multiqubit States with Quantum Technologies

**Authors:** Nataliia Susulovska<sup>1</sup>; Khrystyna Gnatenko<sup>1</sup>

<sup>1</sup> *Professor Ivan Vakarchuk Department for Theoretical Physics, Ivan Franko National University of Lviv*

**Corresponding Author:** n.a.susulovska@gmail.com

Studying the Entanglement of Multiqubit States with Quantum Technologies

The utilization of entangled multiqubit resource states is a cornerstone of practical quantum computing allowing for the development of innovative quantum algorithms, which facilitate computational

advantage over classical approaches. On the other hand, thanks to the recent advancements in quantum technologies, quantum processors can be exploited to model systems of many spins and investigate the properties of their states with quantum programming methods.

Presently, we consider multiqubit states with different types of interaction and study their entanglement both analytically and with the help of quantum computations. The focus is on establishing efficient representations for the classes of quantum states of interest in terms of complex mathematical structures such as graphs, hypergraphs and further determining the relationships between physical properties of such states and geometric properties of the proposed representations. Namely, we examine graph states generated by the action of controlled phase-shift operators on an arbitrary separable state of the multipartite system, which allows us to study bipartite interactions [1], [2]. Subsequently, we consider quantum hypergraph states, which constitute a generalization of graph states permitting the introduction of multipartite interactions via the utilization of hyperedges [3]. In this context, 3-uniform hypergraph states prepared with the help of RZZY gates are investigated in detail. In both cases quantum states represented by graphs or hypergraphs of different connectivity are considered. In order to quantify the entanglement of multiqubit states under investigation we resort to the definition of the geometric measure of entanglement and leverage its relation to the mean spin, a quantity easily measurable on a quantum computer [4]. Analytical expressions for the geometric measure of entanglement of an arbitrary qubit with the remaining system in graph and hypergraph states are derived, which allows us to analyze its dependency on the state parameters. In specific cases the relationship between the geometric measure of entanglement of a qubit and its corresponding vertex degree is obtained. Additionally, we prepare graph and hypergraph states on gated-based quantum devices, namely both IBM's quantum simulator Qiskit Aer and real quantum hardware [5], and detect the associated geometric measure of entanglement based on mean spin measurements. Corresponding quantum computations support or theoretical findings and showcase the capabilities of current quantum computers in the studies of physical systems.

1. Kh. P. Gnatenko and N. A. Susulovska, *EPL* 136(4) (2021).
2. N. A. Susulovska, *Ukr. J. Phys.* 70(3) (2025).
3. M. Rossi, M. Huber, D. Bruß, and M. Macchiavello, *New J. Phys.* 15, 113022 (2013).
4. A. M. Frydryszak, M. I. Samar, and V. M. Tkachuk, *Eur. Phys. J. D* 71, 233 (2017).
5. \*Qiskit Aer Documentation\*, [https://qiskit.github.io/qiskit-aer/getting\\_started.html](https://qiskit.github.io/qiskit-aer/getting_started.html)

## Quantum Technologies, Foundations and Optics / 32

### Meta-fibers: merging nanophotonics and fibers

**Author:** [Oleh Yermakov](#)<sup>1</sup>

<sup>1</sup> V. N. Karazin Kharkiv National University, Kharkiv, Ukraine / Leibniz Institute of Photonic Technology, Jena, Germany

**Corresponding Author:** [oe.yermakov@gmail.com](mailto:oe.yermakov@gmail.com)

Remote collection and analysis of light is highly important for a plethora of applications including spectroscopy, endoscopy, biosensing, quantum communications, etc. Commercial optical fibers are the best platform for this purpose due to their ability to operate in strongly limited and closed spaces (particularly, in-vivo). The payback of this advantage is the low coupling of the incident light into the fiber, especially under oblique incidence.

Here, we propose to overcome this fundamental limitation by enhancing the fiber tips with axial all-dielectric nanostructures. Indeed, we demonstrate the improvement of the light coupling efficiency by several orders of magnitude for the single-mode, multimode and multicore fibers reinforced with polymer concentric nanorings fabricated by direct laser writing approach. We have demonstrated



light collection improvement at multiple selected angles and over large angular intervals. The applications can be found in a variety of cutting-edge fields that require highly efficient remote light collection.

## Quantum Technologies, Foundations and Optics / 34

### Engineering of plasmonic anisotropic nanopatch-based metasurfaces

**Authors:** Artem Hrinchenko<sup>1</sup>; Oleh Demianyk<sup>1</sup>; Sergey Polevoy<sup>2</sup>; Oleh Yermakov<sup>3</sup>

<sup>1</sup> V. N. Karazin Kharkiv National University

<sup>2</sup> O. Ya. Usikov Institute for Radiophysics and Electronics NASU

<sup>3</sup> V. N. Karazin Kharkiv National University, Kharkiv, Ukraine / Leibniz Institute of Photonic Technology, Jena, Germany

**Corresponding Author:** artitus1509@gmail.com

Hyperbolic metasurfaces are known for their dispersion and polarization properties, such as negative refraction, hyperlensing, enhanced spontaneous emission, etc [1]. The surface waves localized at hyperbolic metasurfaces are called hyperbolic plasmon-polaritons and exhibit a lot of potential applications for planar technologies [2].

In this work, we analyze the dependencies of the spectral positions of the resonances and spectral bandwidth of hyperbolic regime for the metasurfaces based on square arrays of the nanodisks [3] and rectangular nanopatches [4]. Namely, we study the resonant characteristics of metasurfaces by varying the size of the nanoparticles, the degree of stretching (anisotropy) and the period of the metasurface from the isotropic to extreme anisotropic cases.

Surface plasmons typically propagate radially in all directions, losing a significant portion of their energy during the directional signal transferring. Typical values of the signal amplitude reaching the receiver usually do not exceed 0.1% of the signal amplitude at the source output, and this significantly limits the use of surface plasmons in practical applications. To solve this problem, we demonstrate the one special regime as plasmon canalization, which is characterized by a flat isofrequency contour and the self-collimated unidirectional propagation of surface wave. In this case, the signal transmission efficiency is close to the maximum, that is, the signal amplitude at the source output and at the receiver input are approximately the same, which makes it possible to ensure highly efficient signal transmission with minimal losses. The canalization takes place in the vicinity of one of the resonances highlighting the relevance of the metasurface engineering for the in-plane optical signal transferring.

1. O. Takayama and A. V. Lavrinenko, *J. Opt. Soc. Am. B: Opt. Phys.* 36(8), 38–48 (2019).
2. J. S. Gomez-Diaz and A. Alù, *ACS Photonics* 3(12), 2211–2224 (2016).
3. A. Hrinchenko and O. Yermakov, *J. Phys. D: Appl. Phys.* 56(46), 465105 (2023).
4. A. Hrinchenko, S. Polevoy, O. Demianyk, and O. Yermakov, *J. Appl. Phys.* 135(22), 223102 (2024).

### Enhancement of chiral sensing with plasmonics meta-gratings

**Authors:** Oleh Demianyk<sup>1</sup>; Sergey Polevoy<sup>2</sup>; Vladimir Tuz<sup>1</sup>; Oleh Yermakov<sup>3</sup>

<sup>1</sup> V. N. Karazin Kharkiv National University

<sup>2</sup> O. Ya. Usikov Institute for Radiophysics and Electronics NASU

<sup>3</sup> V. N. Karazin Kharkiv National University, Kharkiv, Ukraine / Leibniz Institute of Photonic Technology, Jena, Germany

**Corresponding Author:** o.demianyk@gmail.com

Chirality refers to the property of an object that cannot be superimposed on its mirror image. Despite having the same chemical structure, most chiral molecules, also known as enantiomers, exhibit significant differences in biological activity, being either the poison or the drug, depending on their handedness [1]. Detection and separation of chiral molecules are crucial across various fields, including pharmacology, environmental science, and the food industry. The major challenge during the measurement of chiral substances lies in detecting extremely weak chiroptical signals from small concentrations of molecules. Optical plasmonic sensors, based on an angle-resolved surface plasmon resonance, enable precise identification and quantification of the correct isomer in a test substance in a real-time regime [2], which is essential for the safety and efficiency of the pharmaceutical industry, drug testing, and medical applications.

In this work, we study the nanophotonics platform for plasmonic chiroptical sensing based on a thin gold film of 50-nm thickness on the quartz substrate. Exciting a surface plasmon-polariton via the prism coupling in the attenuated total internal reflection regime (Kretschmann configuration [3]) with a plane TM-polarized wave, we study the reflection spectra. In this case, the small response in the TE-polarization emerges due to the mixing of electric and magnetic fields. As a result, there is the angular shift between the spectral resonances in right- and left-handed circular polarized waves due to the presence of the chiral substance.

Then, we structured a thin film over a gold meta-grating to enhance the sensitivity of the chiroptical sensor. We observe the enhancement of the chiral sensitivity by about two orders of magnitude. The observed enhancement is explained by the appearance of Rayleigh's anomaly [4], which arises due to the meta-grating's structure. This phenomenon occurs under specific conditions where a diffracted wave originates and propagates under the grazing angles along the grating surface, becoming an evanescent wave. As a result, the coupling between the evanescent wave strongly localized at the edges of the grating and the chiral substance leads to enhanced light-matter interactions and significant amplification of the chiroptical response.

Thus, we demonstrate that the structuring of the thin plasmonic film leads to the multifold enhancement of the chiral sensing. Subwavelength plasmonic meta-gratings have strong prospects as a nanophotonics platform for detecting, quantifying, and separating low concentrations of chiral molecules. The results obtained open new opportunities for the optical sensing of polarization-sensitive molecules in the real-time regime.

1. L. Warning et al., *ACS Nano* 10(15), 15538 (2021).
2. S. Droulias and L. Bougas, *ACS Photonics* 6(6), 1485 (2019).
3. E. Kretschmann and H. Raether, *Z. Naturforsch. A* 12(23), 2135 (1968).
4. A. A. Maradudin et al., *J. Opt.* 18(2), 024004 (2016).

## Spin-directional coupling in hyperbolic shear metasurfaces

**Authors:** Veronika Batianova<sup>1</sup>; Oleh Yermakov<sup>2</sup>

<sup>1</sup> V. N. Karazin Kharkiv National University, Kharkiv, Ukraine

<sup>2</sup> V. N. Karazin Kharkiv National University, Kharkiv, Ukraine / Leibniz Institute of Photonic Technology, Jena, Germany

**Corresponding Author:** vbatyanova5@gmail.com

The miniaturization and flattening of modern optical devices demand tunable control over highly localized electromagnetic fields. While there is progress in the control of group and phase velocities of localized light, its polarization properties and directivity pattern are still difficult to manage.

Optical spin angular momentum (SAM) defines polarization properties of light [1]. In particular, plane waves possess longitudinal SAM (parallel to the wave propagation direction), while conventional surface plasmon-polaritons at the metal-dielectric interface have purely transverse SAM (perpendicularly to the wave propagation direction). This phenomenon of strict connection between the wave propagation and SAM is known as spin-momentum locking [2], or robust spin-directional coupling [3]. The gap in the SAM manipulation between the purely longitudinal and transverse states limits polarization control and design flexibility in nanophotonic systems. Anisotropic metasurfaces were previously introduced to partially overcome this limitation by enabling hybrid TE-TM polarization modes and extended in-plane spin control via the nanostructures designing [2]. Nevertheless, the possible SAM directions remain limited.

The recent discovery of the shear hyperbolic metasurfaces [4] opens new opportunities for the in-plane SAM manipulation. Shear hyperbolic metasurfaces are two-dimensional (2D) structures engineered to support surface modes of hyperbolic dispersion with frequency-dependent optical axis. They are composed of a periodic array of two orthogonal sets of subwavelength dipole resonators rotated with respect to each other.

In this work, we show that shear hyperbolic metasurfaces provide broader control over the propagation direction and the angle between the SAM and wave propagation direction compared to other two-dimensional anisotropic systems. The improved tunability allows access to a wider range of polarization states and directional spin configurations, making them particularly promising for spin-based photonic applications.

In addition to spin control properties, shear hyperbolic metasurfaces also support canalization regimes, enabling diffractionless, highly directional energy propagation [5]. This dual functionality makes them a promising platform for next-generation photonic and opto-spintronic devices. Their ability to simultaneously route energy and tune polarization and spin states at the nanoscale is essential for the development of compact, highly integrated optical systems.

1. K. Y. Bliokh et al., *Optica* 9(12), 796–808 (2015).
2. T. Van Mechelen and Z. Jacob, *Optica* 3(2), 118–126 (2016).
3. K. Y. Bliokh and F. Nori, *Physics Reports* 592, 1–38 (2015).
4. E. M. Renzi et al., *Phys. Rev. Lett.* 132, 263803 (2024).
5. O. Y. Yermakov et al., *Phys. Rev. B* 94(7), 075446 (2016).

## Physics of Nuclei and Elementary Particles

### Structure of hypernucleus ${}^7_{\Lambda}\text{Li}$ within the three-cluster model

**Author:** Nursultan Kalzhigitov<sup>1</sup>; Victor Vasilevsky<sup>2</sup>

<sup>1</sup> Al-Farabi Kazakh National University

<sup>2</sup> Bogolyubov Institute for Theoretical Physics

**Corresponding Author:** knurto1@gmail.com

Structure and nuclear reactions in hypernuclear systems are highly relevant at present. The increased amount of new experimental data over the past decades supports such interest in these objects. The interaction of the  $\Lambda$  particles with nucleons is responsible for forming light and weakly bound hypernuclei. Among them is the  ${}^7_{\Lambda}\text{Li}$  hypernucleus. One of the interesting features of  ${}^7_{\Lambda}\text{Li}$  is that it has reached the spectrum of bound states (four bound states) among other light hypernuclei. Recall that the ordinary  ${}^7\text{Li}$  nucleus has only two bound states. Besides, in an experiment [1] the

bulk properties of this nucleus have been studied and it was found that a significant decrease of the size of the  ${}^7_\Lambda\text{Li}$  hypernucleus occurred when the  $\Lambda$  hyperon was added to a weakly bound nucleus, such as  ${}^6\text{Li}$ . As the  $\Lambda$  particle is not a subject to the Pauli principle, it can be located in the center of the nucleus, attracting the surrounding nucleons to itself. This, in turn, leads to the compression of the  ${}^7_\Lambda\text{Li}$  nucleus.

In our work, we study the bound and resonant states of the  ${}^7_\Lambda\text{Li}$  hypernucleus within the three-cluster model [2], which uses several three-cluster configurations and oscillator functions to expand wave functions of the inter-cluster interaction. To describe inter-cluster motion and to numerate channels of the three-cluster system, we use hyperspherical coordinates and a large set of hyperspherical harmonics. To achieve a more correct description of the nucleus under study, two three-cluster configurations of the  ${}^7_\Lambda\text{Li}$  nucleus were involved in the calculations:  ${}^4\text{He} + d + \Lambda$ ,  ${}^3\text{He} + {}^3\text{H} + \Lambda$ . These configurations allow a more accurate description of the structure of the  ${}^7_\Lambda\text{Li}$  hypernucleus and the dynamics of its cluster-cluster interaction, such as  $\Lambda + {}^6\text{Li}$ ,  $d + {}^5_\Lambda\text{He}$ ,  ${}^4\text{He} + {}^3\text{H}$ . In our calculations, we use the Hasegawa-Nagata nucleon–nucleon potential [3] and the YNG nucleon–hyperon potential [4], which enables us to correctly reproduce the interaction of nucleons with nucleons and nucleons with the  $\Lambda$  hyperon.

We calculated energies and wave functions of bound states of  ${}^7_\Lambda\text{Li}$ , and determined those channels that give the maximal contribution to the wave function of these states. We also determined the mass root-mean-square radii of the bound states, which indicate that the hypernucleus  ${}^7_\Lambda\text{Li}$  is more compact than the ordinary nucleus. The calculated correlation functions provided information about the most probable relative positions of the interacting clusters. The weights of the functions of a fixed oscillator shell in the wave functions of the bound states of  ${}^7_\Lambda\text{Li}$  unambiguously demonstrate that the lambda hyperon can be located inside the nucleus  ${}^6\text{Li}$  with significant probability. It is also demonstrated that our model reasonably well reproduces existing experimental data for the energies of bound states.

We also studied the phase shifts of so-called 3-to-3 scattering, which describe processes in a three-cluster continuum, and found several resonance states that decay into three fragments (clusters). These results can be considered a prediction of the existence of narrow resonance states and can be used for planning future experiments.

1. K. Tanida et al., Phys. Rev. Lett. 86, 1982 (2001).
2. V. Vasilevsky, A.V. Nesterov, F. Arickx, J. Broeckhove, Phys. Rev. C 63, 034606 (2001).
3. A. Hasegawa, S. Nagata, Prog. Theor. Phys. 45, 1786 (1971)
4. Y. Yamamoto, et al, Prog. Theor. Phys. Suppl. 117, 361 (1994)

## ON INTERACTION OF LAMBDA HYPERON WITH LIGHTEST NUCLEI IN TWO-CLUSTER MODEL

**Authors:** Sabina Amangeldinova<sup>1</sup>; Nursultan Kalzhigitov<sup>1</sup>; Venera Kurmangaliyeva<sup>1</sup>; Victor Vasilevsky<sup>2</sup>

<sup>1</sup> Al-Farabi Kazakh National University

<sup>2</sup> Bogolyubov Institute for Theoretical Physics

**Corresponding Author:** sabinaa247@gmail.com

The study of reaction dynamics in nuclear and hypernuclear systems is one of the most interesting and relatively new areas of modern nuclear physics and astrophysics. Numerous experimental and theoretical investigations in this area provide a deeper understanding of the properties of dense nuclear matter, as well as the structure of unusual objects in interstellar space, such as neutron stars. In this respect, the peculiarities of interaction between a hyperon and a nucleon are of significant particular importance. Recall that hyperons are baryons containing one or more strange quarks, and their interaction with nucleons has a significant impact on the internal structure of high-density matter, including neutron stars. Depending on the characteristics of the strength of this interaction, a neutron star may become a hyperon star, or a kaon condensate is more likely to form inside it.

These facts stimulate the applications of different theoretical models to understand the structure of light hypernuclei and their interactions.

This research is devoted to the study of discrete and continuous energy spectra of the lightest hypernuclei —  ${}^2_{\Lambda}\text{H}$ ,  ${}^3_{\Lambda}\text{H}$ ,  ${}^4_{\Lambda}\text{H}$ , and  ${}^5_{\Lambda}\text{He}$ . These hypernuclei were considered as two-cluster configurations:  $\Lambda + p$ ,  $\Lambda + d$ ,  $\Lambda + {}^3\text{H}$ , and  $\Lambda + {}^4\text{He}$ , respectively. We also studied ordinary nuclei  ${}^2\text{H}$ ,  ${}^3\text{H}$ ,  ${}^4\text{H}$ , and  ${}^5\text{He}$  formed by interaction of neutrons with protons, deuterons, and nuclei  ${}^3\text{H}$  and  ${}^4\text{He}$ , respectively. This allows us to reveal and understand peculiarities of the hypernuclei. To describe such nuclei and hypernuclei, we employ the algebraic version of the resonating group method (RGM) [1]. This method is based on solving the Schrödinger many-particle equation in matrix form by using the basis of orthonormal oscillator functions.

In the present study, the Hasegawa-Nagata potential [2] and the YNG potential [3] were used to describe nucleon–nucleon and hyperon–nucleon interactions, respectively. The present model with such potentials allows us to correctly describe the energy of bound states of hypernuclei  ${}^3_{\Lambda}\text{H}$ ,  ${}^4_{\Lambda}\text{H}$ , and  ${}^5_{\Lambda}\text{He}$ . Our analysis confirmed that there is no bound state in the  ${}^2_{\Lambda}\text{H}$  hypernucleus, since the weak interaction of the lambda hyperon with the proton and neutron. We determined the mass root-mean-square radius and average distance between the lambda hyperon and the s-shell nucleus. These quantities indicate that the hypernuclei of interest are weakly bound systems with a large distance between the lambda hyperon and the nucleus. It was found that  ${}^2_{\Lambda}\text{H}$ ,  ${}^3_{\Lambda}\text{H}$ ,  ${}^4_{\Lambda}\text{H}$ , and  ${}^5_{\Lambda}\text{He}$ , contrary to ordinary nuclei, have no resonance states in the two-cluster continuum.

The results obtained in this work will be used to study hypernuclei  ${}^6_{\Lambda}\text{Li}$ ,  ${}^7_{\Lambda}\text{Li}$ , and  ${}^8_{\Lambda}\text{Li}$  within a three-cluster microscopic model.

1. G.F. Filippov, I.P. Okhrimenko, Sov. J. Nucl. Phys., 32 (1981), p. 480.
2. A. Hasegawa, S. Nagata, Prog. Theor. Phys. 45 (1971), p. 1786.
3. Y. Yamamoto, et al, Prog. Theor. Phys. Suppl., 117, (1994), p. 361.

## Loop Divergences in the Effective Theory of Chern–Simons Boson–Fermion Couplings

**Author:** Oleksandr Khasai<sup>1</sup>; Volodymyr Gorkavenko<sup>2</sup>; Yuliia Borysenkova; Ivan Hrynchak; Mariia Tsarenkova<sup>2</sup>

<sup>1</sup> Bogolyubov Institute for Theoretical Physics of the National Academy of Sciences of Ukraine

<sup>2</sup> Taras Shevchenko National University of Kyiv

**Corresponding Author:** khasaisasha@gmail.com

Although the Standard Model (SM) has proven remarkably effective in accounting for a wide range of experimental data from particle colliders, it remains an incomplete framework. It does not account for several key phenomena, such as the oscillations of active neutrinos, the observed matter–antimatter imbalance in the Universe, and the nature of dark matter. Consequently, the SM requires extensions that introduce new particles and fundamental interactions.

One explanation for why these hypothetical particles have eluded detection is that they are either very massive with weak couplings to SM particles or very light but interact so feebly that their presence is difficult to observe. In the case of heavy particles, future high-energy colliders like the FCC may have sufficient reach to detect them. Conversely, if these particles are light, they could potentially be discovered at existing facilities in experiments operating at the intensity frontier—such as MATHUSLA, FACET, FASER, SHiP, and others at CERN.

Here we investigate a specific extension of the SM that introduces a new massive vector boson, known as the Chern–Simons (CS) boson, which interacts through terms analogous to the Chern–Simons structure. These interactions are encapsulated by a minimal, gauge-invariant Lagrangian constructed from dimension-six operators {1}:

$$\mathcal{L}_1 = \frac{C_Y}{\Lambda_Y^2} \cdot X_\mu (\mathfrak{D}_\nu H)^\dagger H B_{\lambda\rho} \cdot \epsilon^{\mu\nu\lambda\rho} + h.c., \quad (1)$$

$$\mathcal{L}_2 = \frac{C_{SU(2)}}{\Lambda_{SU(2)}^2} \cdot X_\mu (\mathfrak{D}_\nu H)^\dagger F_{\lambda\rho} H \cdot \epsilon^{\mu\nu\lambda\rho} + h.c., \quad (2)$$

In these expressions,  $\Lambda_Y$  and  $\Lambda_{SU(2)}$  denote new energy thresholds associated with physics beyond the SM, and  $C_Y$ ,  $C_{SU(2)}$  are dimensionless coupling constants. The Levi-Civita symbol  $\epsilon^{\mu\nu\lambda\rho}$  is defined with  $\epsilon^{0123} = +1$ . The vector field  $X_\mu$  corresponds to the CS boson, while  $H$  is the Higgs doublet scalar field. The field strength tensors  $B_{\mu\nu}$  and  $F_{\mu\nu}$  describe the dynamics of the  $U(1)_Y$  and  $SU(2)_W$  gauge fields of the SM, respectively.

After electroweak symmetry breaking, the interactions defined by Lagrangians (1) and (2) give rise to additional terms in the effective theory, including three-particle interactions characterized by dimension-four operators:

$$\mathcal{L}_{CS} = c_z \epsilon^{\mu\nu\lambda\rho} X_\mu Z_\nu \partial_\lambda Z_\rho + c_\gamma \epsilon^{\mu\nu\lambda\rho} X_\mu Z_\nu \partial_\lambda A_\rho + \{c_w \epsilon^{\mu\nu\lambda\rho} X_\mu W_\nu^- \partial_\lambda W_\rho^+ + h.c.\}, \quad (3)$$

Here,  $A_\mu$  is the photon field, while  $W_\mu^\pm$  and  $Z_\mu$  denote the charged and neutral weak gauge bosons, respectively. The coefficients  $c_z$  and  $c_\gamma$  are real-valued constants, whereas  $c_w$  may generally be complex. Importantly, in this minimal scenario, the CS boson  $X_\mu$  does not couple directly to matter fields.

Effective loop interactions involving the CS boson and fermions of different flavors are well-behaved and finite. This finiteness arises because any potential divergence is tied to off-diagonal terms in the matrix product  $(V^\dagger V)_{ij}$ , where  $V$  represents the CKM matrix. These terms vanish, eliminating problematic contributions, as previously demonstrated in [2,3].

However, complications emerge in the case where the CS boson interacts with fermions of the same generation. Our prior work [4] explored this scenario within the unitary gauge, using a purely four-dimensional interaction basis defined by (3). The findings revealed persistent divergences in loop diagrams, which could not be eliminated by conventional means.

In the present work [5], we extend the investigation to the more general  $R_\xi$  gauge, allowing for arbitrary but finite values of the gauge-fixing parameters  $\xi_i$ , and concentrate on the CS boson's loop interactions with same-flavor leptons.

Our analysis shows that even when all one-loop diagrams are considered in this gauge setting, ultraviolet divergences persist. As a result, the seemingly renormalizable theory defined by (3) fails to meet renormalizability requirements in the presence of a massive vector field.

Analysing the sum of the divergent parts of all considered diagrams, we identify two divergent terms for the CS boson interacting with same-flavor fermions that are present in both the unitary and  $R_\xi$  gauge calculations. Since the initial interaction of the CS bosons with SM fields is given by dimension-6 operators (1) and (2), we conclude that after the electroweak symmetry breaking the interaction of the CS boson with fermions of the same flavor should be considered within the framework of the effective field theory approach and can be written as

$$\mathcal{L}_{Xff}^{int} = \bar{f} \gamma^\mu (\alpha_f + \beta_f \gamma^5) f X_\mu + \frac{m_f}{v^2} \bar{f} \sigma^{\mu\nu} (\gamma_f + \delta_f \gamma^5) f X_{\mu\nu} + \mathcal{L}'_{Xff}, \quad (4)$$

where  $X_{\mu\nu} = \partial_\mu X_\nu - \partial_\nu X_\mu$ . Here dimensionless parameters  $\alpha_f$ ,  $\beta_f$ ,  $\gamma_f$ ,  $\delta_f$  should be considered as new 4 parameters of the effective theory and  $\mathcal{L}'_{Xff}$  is a well-defined Lagrangian of interaction depending on the coupling parameters of the Lagrangian (3).

#### Acknowledgments:

The work of V.G., I.H., and O.Kh. was supported by the National Research Foundation of Ukraine under project No. 2023.03/0149. The work of O.Kh. was funded by the Simons Foundation. The authors are grateful to Eduard Gorbar for fruitful discussions and helpful comments.

1. I. Antoniadis, A. Boyarsky, S. Espahbodi, O. Ruchayskiy, and J. D. Wells. Anomaly driven signatures of new invisible physics at the Large Hadron Collider. Nucl. Phys. B, 824:296–313, 2010.
2. J. A. Dror, R. Lasenby, and M. Pospelov. Dark forces coupled to nonconserved currents. Phys. Rev. D, 96(7):075036, 2017.
3. Y. Borysenkova, P. Kashko, M. Tsarenkova, K. Bondarenko, and V. Gorkavenko. Production of Chern–Simons bosons in decays of mesons. J. Phys. G, 49(8):085003, 2022.

4. Y. Borysenkova, V. Gorkavenko, I. Hrynychak, O. Khasai, and M. Tsarenkova. Divergences in the effective loop interaction of the Chern-Simons bosons with leptons. The unitary gauge case. *Ukr. J. Phys.*, 69:897, 2024.
5. Y. Borysenkova, V. Gorkavenko, I. Hrynychak, O. Khasai, and M. Tsarenkova. Divergences in the effective interaction between Chern-Simons bosons and fermions. *arXiv:2505.12550*, 2025.

## Induced Vacuum Magnetic Flux in the Background of a Linear Topological Defect. The case of fermion matter

**Author:** Yullia Pylypchuk<sup>1</sup>; Pavlo Nakaznyi<sup>2</sup>; Volodymyr Gorkavenko<sup>3</sup>

<sup>1</sup> *Educational and Research Institute of Physics and Technology, National Technical University of Ukraine \ «Igor Sikorsky Kyiv Polytechnic Institute*

<sup>2</sup> *Educational and Research Institute of Physics and Technology, National Technical University of Ukraine «Igor Sikorsky Kyiv Polytechnic Institute»*

<sup>3</sup> *Faculty of Physics, Taras Shevchenko National University of Kyiv*

**Corresponding Author:** y.pylypchuk-ipt@lil.kpi.ua

In many theoretical models describing the evolution of the early Universe, topological defects appear, in particular in the form of magnetic cosmic strings [1]. String models are used not only in the physics of the early Universe, but also in the physics of hadrons and continuous media. In particular, structures analogous to cosmic strings arise in the theory of superconductivity. Here, they are associated with Abrikosov vortices - tubes of magnetic flux in superconductors of the second kind at a temperature below the critical temperature.

We will consider a model of the topological defect (magnetic cosmic string) as an impenetrable for the fermion matter field tube with a magnetic field inside. A certain boundary condition must be imposed on the surface of the magnetic tube, which is impermeable to the fields, to model the cosmic string. The peculiarity of fermionic matter is that this boundary condition cannot be the usual Neumann, or Dirichlet, or Robin condition. In this case, the condition of self-adjointness of the Dirac Hamiltonian should be applied.

An important effect is the induction of a magnetic flux outside the magnetic cosmic string in the vacuum of fermion matter. Theoretical study of this process allows one to constrain the values of boundary conditions parameters. Since analytical solutions for this process are extremely complex, numerical modelling is necessary for their analysis, which is the subject of this work.

It has been shown previously that in  $2 + 1$  space-time [2], a straight magnetic cosmic string of nonvanishing transverse size induces a magnetic field in the vacuum of the quantum relativistic charged spinor matter field. The corresponding analytical dependencies for the induced magnetic flux were obtained for  $3 + 1$  space-time [2]. However, the analytical dependencies, which are quite complex for analysis even in  $2 + 1$  space-time, in the case of generalization to 3 spatial dimensions, become prohibitively complex for direct calculation and analysis. Therefore, the analysis of the obtained dependencies and the exclusion of non-physical boundary conditions on their basis is an independent problem for numerical calculations.

Directly integrating the corresponding expression has shown to be highly challenging due to its complexity, so it was decided to find a similar function that would be easier to integrate. To do this, we first find the interpolation function and then extrapolate it. As a result, we investigate the induced magnetic flux in the vacuum of a fermionic field in the background of a magnetic cosmic string, and compute it. For the case of boundary condition self-adjoint extension parameter  $\theta = 0$ , it was shown that the induced magnetic flux in  $(3 + 1)$ -dimensional space-time (in dimensionless units) is significantly larger than in  $(2 + 1)$  dimensions for small values of the tube radius, specifically with tube thickness  $mr_0 < 0.16$ , see Fig.1.

The requirement that the total induced vacuum flux be finite restricts the set of admissible boundary conditions to a single choice: the MIT bag boundary condition, self-adjoint extension parameter

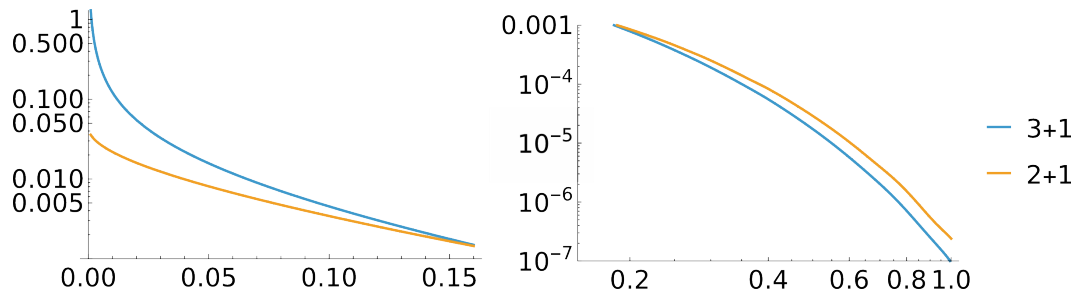


Figure 1: Induced vacuum magnetic flux in dimensionless units in 2+1 space-time ( $em^{-1}\Phi_I^{(d=2)}$ ) and in 3+1 space-time ( $e\pi\Phi_I^{(d=3)}$ ) as a function of the tube thickness ( $mr_0$ ) for the case of the boundary-condition self-adjoint extension parameter  $\theta = 0$ .

$\theta = 0$ . In contrast, the case  $\theta = \pi$ , which yields a finite induced magnetic flux in  $(2+1)$ -dimensional space-time, leads to an infinite induced flux in  $(3+1)$  dimensions. All other values of the self-adjoint extension parameter  $\theta$  are nonphysical and lead to infinite induced magnetic flux in the vacuum of the fermion matter field.

1. A. Vilenkin and E.P.S. Shellard, *Cosmic Strings and Other Topological Defects* (Cambridge Univ. Press, Cambridge UK, 1994).
2. Yu.A. Sitenko and V.M. Gorkavenko, *Induced vacuum magnetic flux in quantum spinor matter in the background of a topological defect in two-dimensional space*, Phys. Rev. D 100, 085011 (2019).
3. Yu.A. Sitenko, *Induced vacuum magnetic field in the cosmic string background*, Phys. Rev. D 104, 045013 (2021).

## Integrated HydroKinetic Model at Relativistic Heavy Ion Collider Energies

**Authors:** Musfer Adzhymambetov<sup>1</sup>; Yuri Sinyukov<sup>1</sup>

<sup>1</sup> Bogolyubov Institute for Theoretical Physics

**Corresponding Author:** adzhymambetov@gmail.com

Understanding the phase structure of strongly interacting matter is a central goal of ongoing and future heavy-ion experiments, such as RHIC's Beam Energy Scan (BES) and FAIR's Compressed Baryonic Matter (CBM) program. These efforts aim to explore the Quantum Chromodynamics (QCD) phase diagram at high baryon densities, where a critical point and a first-order phase transition are conjectured to exist. To support the interpretation of experimental data, we have developed a new theoretical framework [1] extending the integrated hydrokinetic model (iHKM) [2] to the lower collision energies relevant for these programs. This model allows for dynamical simulations using different equations of state, both with and without a phase transition. In this talk, I will present our first results for the RHIC BES energy range, comparing model predictions with experimental data. Our findings suggest hints of a phase transition at lower collision energies, while a crossover behavior remains more consistent with observables at higher energies.

1. M. Adzhymambetov, Y. Sinyukov, arXiv:2412.00458 [hep-ph] (2024).
2. V. M. Shapoval, M. D. Adzhymambetov, Yu. M. Sinyukov, Eur. Phys. J. A 56 (2020) 260, [arXiv:2006.16697 [nucl-th]], <https://doi.org/10.1140/epja/s10050-020-00266-x>.



## A question concerning phase transitions in a pion system of particles and antiparticles

**Authors:** Vladyslav Karpenko<sup>1</sup>; Dmytro Anchyskin<sup>2</sup>; Denys Zhuravel<sup>1</sup>; Volodymyr Gnatovskyy<sup>1</sup>

<sup>1</sup> Bogolyubov Institute for Theoretical Physics of the National Academy of Sciences of Ukraine

<sup>2</sup> Bogolyubov Institute for Theoretical Physics of the National Academy of Sciences of Ukraine, FIAS

**Corresponding Author:** karpych1717@gmail.com

The thermodynamic properties of an interacting pion system composed of particles and antiparticles are studied at finite high temperatures and densities, which may arise in relativistic collisions of individual particles and entire atomic nuclei. Systems containing both particles and antiparticles are considered under the condition of isospin (charge) density conservation. The results are obtained within a Skyrme-like mean-field thermodynamic model. The mean field depends on the total particle density and includes both attractive and repulsive components. Phase diagrams are constructed, illustrating in particular the effect of the attractive interaction on the phase structure of the system.

## Systematic Investigation of Density Fluctuations in Laser Wake-field Accelerators on the Properties of the Accelerated Electrons

**Author:** Yurii Perets<sup>1</sup>; Richard Pausch<sup>2</sup>

<sup>1</sup> Nuclear and High Energy Physics Department

<sup>2</sup> Helmholtz-Zentrum Dresden-Rossendorf

**Corresponding Author:** yuraperets2@gmail.com

Fundamental questions on the nature of matter and energy have found answers thanks to the use of particle accelerators. However, the accelerating field in superconducting radio-frequency cavities due to electrical breakdown is limited to about 100 MV/m. This limits the amount of acceleration over any given length, requiring very long accelerators to reach high energies. To overcome this limitation, novel acceleration techniques are being explored, including plasma wakefield acceleration, that can exceed an accelerating gradient of  $E > 100$  GV/m.

Until now, almost all Laser Wakefield Acceleration (LWFA) simulations have assumed smooth plasma density profiles, but recent few-cycle shadowgraph imaging of the acceleration process has revealed small density fluctuations in the plasma profile. The main focus of this project is on a simulation study of the nonlinear laser-plasma interaction using the particle-in-cell code PICongPU, and based on measured density profiles, we want to determine the difference in electron beam quality after the LWFA process caused by the non-smooth density.

## High-order cumulants near the critical point from molecular dynamics

**Authors:** Volodymyr Kuznietsov<sup>1</sup>; Volodymyr Vovchenko<sup>1</sup>; Mark Gorenstein<sup>2</sup>; Volker Koch<sup>3</sup>

<sup>1</sup> University of Houston

<sup>2</sup> Bogolyubov Institute for Theoretical Physics, National Academy of Sciences of Ukraine

<sup>3</sup> Lawrence Berkeley National Laboratory (LBNL)

**Corresponding Author:** kuznietsov09@ukr.net

We calculate non-Gaussian cumulants of particle number near the 3D-Ising critical point by means of GPU-accelerated molecular dynamics simulations. We perform ensemble averaging with large statistics, and study the equilibration of cumulants near the critical point. We find that scaled variance, skewness, and kurtosis reflect the expected critical behavior of fluctuations and equilibrate on comparable time scales. We also incorporate Bjorken-like collective flow model to study the behavior of non-Gaussian fluctuations in the rapidity space. The results are put in the context of measurements of cumulants and factorial cumulants of protons in heavy-ion collisions at RHIC.

## Femtoscopy of rotating sources

**Author:** Oleh Savchuk<sup>1</sup>

<sup>1</sup> *Facility for Rare Isotope Beams*

**Corresponding Author:** savchukolegv@gmail.com

In heavy-ion collisions, as two nuclei go through each other and form hot and dense matter they also transfer some of the angular momentum to the fireball, resulting in the non-zero vorticity. The connection between the initial-state, equation of state and vorticity exists and is of special interest. In this case coarse-graining of non-central Au+Au heavy-ion collisions at  $E_{lab} = 1.23$  AGeV is performed in order to extract collective velocity as a function of position and time. The rotation modifies space-time picture of particle emission leading to profound consequences for proton-pion femtoscopic correlations. A novel approach to extract source functions of a rotating system from correlation functions is presented and distance between proton and pion emission centers are used as a quantity related to the strength of rotation. Thus a new way to measure vorticity is obtained.

## Search for hidden particles in intensity frontier experiments

**Author:** Volodymyr Gorkavenko<sup>1</sup>

<sup>1</sup> *Taras Shevchenko National University of Kyiv*

**Corresponding Author:** gorkavol@gmail.com

Despite the undeniable success of the Standard Model of particle physics (SM), there remain several phenomena, such as neutrino oscillations, the baryon asymmetry of the Universe, and dark matter, that the SM fails to explain. These phenomena clearly indicate the need for an extension of the SM, most likely involving new particles beyond its current framework. However, there is also a possibility that there are new particles in hidden sectors of the SM unrelated to solving these problems.

Numerous experiments are being conducted in the search for new physics, and they are generally categorized into two main approaches: the energy frontier and the intensity frontier. The energy frontier involves attempts to directly produce and detect heavy new particles at high-energy accelerators. In contrast, the intensity frontier focuses on the production and detection of light new particles that interact only feebly with Standard Model particles.

This work discusses the future SHiP (Search for Hidden Particles) experiment at the CERN SPS, which belongs to the intensity frontier program. The advantages and technical features of the SHiP experiment are outlined.

## Condensed Matter and Statistical Theory of Many-body Systems

### Longitudinal Josephson effect in bilayer systems with electron-hole pairing

**Authors:** Oleksandr Konstantynov<sup>1</sup>; Sergiy Shevchenko<sup>2</sup>

<sup>1</sup> *B.Verkin Institute for Low Temperature Physics and Engineering of the National Academy of Sciences of Ukraine*

<sup>2</sup> *B. Verkin ILTPE of NASU*

**Corresponding Author:** akonstantinov@ilt.kharkov.ua

The study investigates non-dissipative longitudinal current states in bilayer systems with pairing of spatially separated electrons and holes in the presence of a potential barrier that divides the system into two macroscopic regions. The longitudinal current flowing across this barrier is identified as the longitudinal Josephson effect, while the current between the electron and hole layers across the insulating interlayer is termed the transverse Josephson current. In practical experimental setups, the transverse current can be made negligible, and is therefore neglected in this study.

The analysis reveals that the longitudinal current's dependence on the tunneling matrix elements is strongly influenced by the system's density. In high-density systems, where the size of the electron-hole pairs greatly exceeds the average inter-pair distance, the current is proportional to the product of the tunneling matrix elements in the electron and hole layers. This means then for the longitudinal Josephson effect to occur in a high-density electron-hole bilayer system, the presence of weak coupling in both layers is required. In contrast, in low-density systems, the current is inversely proportional to the sum of the heights of the potential barriers. This result implies that in a low-density limit even in the absence of a barrier in one of the layers, the longitudinal Josephson effect will still occur due to the strong coupling of the pair components.

The obtained results demonstrate that non-dissipative electric currents can flow through a potential barrier in bilayer systems with pairing of spatially separated electrons and holes.

### Viscoelastic response and anisotropic hydrodynamics in Weyl semimetals

**Author:** Arsen Herasymchuk<sup>1</sup>; Eduard Gorbar<sup>2</sup>; Pavlo Sukhachov<sup>3</sup>

<sup>1</sup> *Bogolyubov Institute for Theoretical Physics*

<sup>2</sup> *Taras Shevchenko National University of Kyiv; Bogolyubov Institute for Theoretical Physics*

<sup>3</sup> *Department of Physics and Astronomy, University of Missouri*

**Corresponding Author:** arsengerasymchuk@gmail.com

We study viscoelastic response in Weyl semimetals with broken time-reversal symmetry. The principal finding is that topology and anisotropy of the Fermi surface are manifested in the viscoelasticity tensor of the electron fluid. In the dynamic (interband) part of this tensor, the anisotropy leads to a qualitatively different, compared with isotropic models, scaling with frequency and the Fermi energy. The components of the viscosity tensor determined by the Fermi-surface properties agree in the Kubo and kinetic formalisms; the latter, however, misses the anomalous Hall viscosity originating from filled states below the Fermi surface. The anisotropy of the dispersion relation is also manifested in the acceleration and relaxation terms of the hydrodynamic equations providing means to probe the anisotropy in transport experiments.

## Tunnel magnon transfer through a ferromagnetic chain

**Author:** Serhii Tunyk<sup>1</sup> E. G. Petrov<sup>1</sup>

<sup>1</sup> *Bogolyubov Institute for Theoretical Physics*

**Corresponding Author:** toonik@ukr.net

In connection with the development of quantum technologies, special attention has been paid to the study of quantum properties of hybrid systems based on magnonics [1]. One of the areas of use of magnons (spin excitations) may be related to transfer of information. The development of quantum information technologies has shown that charged particles are not very convenient for transmitting information. This is due to the Joule heat that is released in the device during the transport of the charge. Therefore, uncharged carriers are most suitable for transmitting information over nanoscale distances. It is proposed to use spin excitations of ordered paramagnetic ions as these. Since the motion of magnons can be controlled by both amagnetic field (acting on the magnetic moment of the paramagnetic ion) and an electric field (through deformation of the crystal field of the ligands), this makes magnons suitable for use in quantum communications. It is also known that magnons interact quite well with phonons and photons – respectively, quanta of oscillations of atomic nuclei and quanta of the electromagnetic field. Based on this fact, it was possible to create hybrid devices that are microcavities with nanomagnets inserted into them. In such hybrid photon-magnon resonators, electromagnetic oscillations occur with frequencies of the order of gigahertz and terahertz, which also corresponds to the excitation frequencies of static (Kitel's) magnons. This opens up wide opportunities for generating one type of excitation quanta into quanta of another type for the purpose of using hybrid photon-magnon resonators in quantum technology. In the work [2] a physical mechanism for implementing quantum communication between photon-magnon resonators is proposed, according to which magnons generated in the nanomagnet of one of the resonators (A or B) can be transferred to the other resonator through ferromagnetic nanoscale chains (see Fig. 1). Such transfer can be carried out in two ways, namely by sequential magnon hoppings along all units of the chain, as well as by magnon tunneling between its terminal units a and b. Here we present the results of theoretical studies of the dependence of rate  $K_{\text{tun}} \sim R(N, \alpha)$  of non-resonant (Fig. 2a) and resonant (Fig. 2b) tunneling of a magnon between nanomagnets A and B connected by a ferromagnetically ordered chain of  $N$  identical units. In the non-resonant tunneling mode, an exponential decrease in rate is clearly visible with increasing  $N$ . The situation changes dramatically in the case of resonant tunneling. In the non-resonant tunneling mode, an exponential decrease in rate is clearly visible with increasing  $N$ . The situation changes dramatically in the case of resonant tunneling. One can see significant changes in rate at certain values of the spin excitation energy entering the chain. In fact, these values will coincide with the broadened magnon energies in the chain. Thus, the tunneling transport of magnons through bridging ferromagnetic structures indicates a specific coherent mechanism for implementing quantum communications using uncharged carriers. Switching the tunneling mode of magnons by a magnetic field can be considered as an effective tool for controlling the transfer of information between ferromagnetic nanocenters.

1. D. Lachance-Quirion, Yu. Tabuchi, A. Gloppe, K. Usami, Ya. Nakamura, J. Appl. Phys. Express 12, 070101 (2019).
2. E. G. Petrov, J. Appl. Phys. 135, 134301 (2024).

## Manipulating domain wall mobility by cross section tailoring in ferromagnetic nanostripes

**Authors:** Dmytro Karakuts<sup>1</sup>; Kostiantyn V. Yershov<sup>2</sup>; Denis D. Sheka<sup>1</sup>

<sup>1</sup> *Taras Shevchenko National University of Kyiv, 01601 Kyiv, Ukraine*

<sup>2</sup> *Leibniz-Institut für Festkörper- und Werkstofforschung, IFW Dresden, 01171 Dresden, Germany*

Manipulation of nanoscale ferromagnetic stripes' magnetic structure can play a pivotal role in the development of high-density, ultrafast magnetic memory and offers a significant potential to enhance the performance of spintronic devices [1,2].

This work is devoted to the theoretical and numerical study of the domain wall motion in straight ferromagnetic nanostripes with variable cross section in the presence of an external magnetic field. It was already shown that the cross-section gradient in a ferromagnetic nanostripe creates a driving force for a domain wall motion [3,4]. However, earlier studies did not account for the potential presence of an external magnetic field, which is necessary for both experimental confirmation of the results and practical applications. Here, we analyze the interaction and competition of the effects caused by the cross-section gradient and the external magnetic field on the domain wall dynamics in a ferromagnetic nanostripe.

The behaviour of the magnetization in a ferromagnetic nanostripe with variable cross section is investigated using the micromagnetic framework introduced in [4]. In this study, we apply the collective variable approach to describe the domain wall. To derive the equations of motion for the collective variables, we employ the Lagrange-Rayleigh formalism, incorporating the spatial variation of the cross-sectional area into both the Lagrangian and the dissipative function.

This study examines the magnetic properties of two distinct nanostripe geometries: one with a localized constriction (Fig. 1a) and another — a wedge-shaped nanostripe (Fig. 2a). For each case, we derive the equation of domain wall motion under the influence of an external magnetic field.

We demonstrate that the cross-section gradient creates an internal driving force, which, under certain conditions, counteracts the external magnetic field's influence on the domain wall. This results in the formation of a new pinning position, with its value calculated for both geometries. The linear dynamics near the pinning position are analyzed, and it is shown that in both geometries, small deviations from the pinning position give rise to damped oscillations.

We also show that for sufficiently large values of the external magnetic field, the domain wall depinning occurs, with the critical depinning field value  $h_d$  being found for both geometries. Additionally, magnetization hysteresis curves are obtained for both geometries, providing a basis for experimental validation of the theoretical predictions (Figs. 1b and 2b). On top of that, the modification of the inertial (Döring) domain wall mass by the cross section variation is found for both cases for small deviations from the pinning position and the absence of damping. All analytical predictions are validated by the full-scale N MAG micromagnetic simulations [5].

While the focus of this work is primarily on the interplay between cross-sectional area gradient and external magnetic field, the model developed also enables the extension of these findings to account for the combined effects of curvature and variable cross section. This research was supported by DFG via Grant No. MC 9/22–1.

1. *Curvilinear Micromagnetism: From Fundamentals to Applications*, edited by D. Makarov and D. Sheka, Topics in Applied Physics Vol. 146 (Springer, Cham, 2022).
2. D. D. Sheka, O. V. Pylypovskyi, O. M. Volkov, K. V. Yershov, V. P. Kravchuk, and D. Makarov, *Small* 18, 2105219 (2022).
3. D. Karakuts, K. V. Yershov, D. D. Sheka, *Functional Magnetic and Spintronic Nanomaterials*, P. 133-145, (Springer, 2024).
4. K. V. Yershov, D. D. Sheka, *Phys. Rev. B* 107, L100415 (2023).
5. T. Fischbacher, M. Franchin, G. Bordignon and H. Fangohr, *IEEE Transactions on Magnetics*, Vol. 43, No. 6, (2007).

## MODELING OF THREE-COMPONENT MULTI-PARTICLE DISCRETE CONGLOMERATIONS

**Authors:** Георгій Кудашкін<sup>1</sup>; Олег Герасимов<sup>1</sup>

<sup>1</sup> *Одеський університет ім. І.І.Мечнікова***Corresponding Author:** rocksoul95@ukr.net

On the way to modeling composite structures consisting of discrete conglomerations containing special impurities in order to create materials with predictable properties, the study of the relationships between microscopic (structural) parameters and macroscopic properties plays a key role. For example, the compressibility of granular media (as well as molecular solutions) is one of the key characteristics that determine their mechanical and thermodynamic properties. In binary mixtures of solid balls described by the Kirkwood-Buff equations and the modified Carnahan-Starling-Mansouri (CSM) equations [1,4,5], specific states of bi-component systems are observed in which, due to the predominant concentration of particles with small or large sizes, the system as a whole demonstrates different types of behavior in terms of compressibility. The influence of the third component on the formation of states with maximum compaction and the compressibility behavior of the system remains an open question [2,3].

This work is devoted to the study of the properties of dense polydisperse mixtures of solid particles using models of the "solid spheres" type and is aimed at investigating the effect of the third component on the compressibility of a multi-particle mixture. The aim is to quantitatively analyze changes in the behavior of compressibility  $\beta T$  when a third component is added to a two-component system with a subsequent change in the relative sizes of all three components.

Particular attention is paid to identifying the conditions for the formation of maximally compacted states that correspond to the minimums of  $\beta T$ . In this way, criteria in terms of mole fractions and relative sizes of components of the formation of states with extreme packing and non-monotonic compressibility behavior are established.

#### REFERENCES

1. Mansoori G. A., Carnahan N. F., Starling K. E., Leland T. W. Equilibrium thermodynamic properties of the mixture of hard spheres // J. Chem. Phys., 1971, Vol. 54, p. 1523-1525.  
<https://doi.org/10.1063/1.1675048>.
2. Gerasymov O. I. Physics of granular materials: a monograph. Odesa: TES, 2015, 264 p.
3. Gerasymov OI, Spivak AY, Sidletska LM Physical mechanisms of processes on which technologies for cleaning and decontamination of contaminated systems are based: monograph. Odesa : Odesa State Environmental University, 2024, 98 p. Access mode: <http://eprints.library.odeku.edu.ua/id/eprint/13061/1/gera>
4. Gerasymov O. I., Spivak A. Y. Some problems of soft matter physics: monograph / Odesa State Ecological University: Helvetica Publishing House, 2020, 200 p. ISBN 978-966-992-202-1. Access mode:  
<http://eprints.library.odeku.edu.ua/id/eprint/9015/>.
5. Gerasymov O. Theoretical Models of Composite Materials for the Protection Technologies // E3S Web of Conferences, 2024, Vol. 477, p. 00008 (8 pages). International Conference on Smart Technologies and Applied Research (STAR'2023), Istanbul, Turkey, October 29-31, 2023.  
<https://doi.org/10.1051/e3sconf/202447700008>.
6. Kang M., Smith P. E. Kirkwood-Buff theory of four and higher component mixtures // J. Chem. Phys., 2008, Vol. 128, p. 244511. DOI: 10.1063/1.2943318.

## Graphene phonons revisited

**Authors:** Dmytro Melnykov<sup>1</sup>; Oleksandr Ponomarov<sup>2</sup>; Svitlana Ponomarova<sup>2</sup>; Yuri Koval<sup>2</sup>; Serhii Kedrovsky<sup>2</sup>

<sup>1</sup> *National Technical University of Ukraine "Igor Sikorsky Kyiv Polytechnic Institute"*

<sup>2</sup> *G.V. Kurdyumov Institute for metal physic of the N.A.S. of Ukraine*

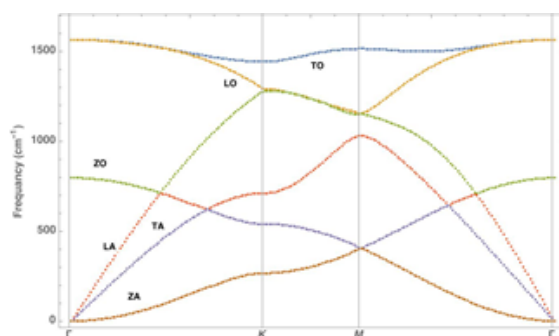


Figure 2: Graphene phonon dispersion for interatomic force constants taken from [2]. Phonon frequency in  $\text{cm}^{-1}$ . The locations of the high symmetry points are  $\Gamma(0., 0., 0.)$ ,  $M(\pi/(a\sqrt{3}), \pi/a, 0.)$ ,  $K(0., 4\pi/(3a), 0.)$ .

**Corresponding Author:** melnykov.dmytro@lil.kpi.ua

We calculated phonon dispersion for graphene with taken into consideration different numbers of nearest neighbors in the Born-von Karman model [1]. Values of force constants were taken from [2-3]. It was shown that quadratic dependence of ZA mode, predicted at [4], depends on set of interatomic force constants and not on number of nearest neighbors, as thought earlier [3]. Our results are in good correspondence with known experimental [5], ab initio [6] and IFC's models [2-3] and could be used for building vibrational thermodynamic model [7] of graphene lattice.

#### References:

1. P. Brüesch, Phonons: Theory and Experiments I, Springer Berlin, Heidelberg, 1982
2. L. J. Karssemeijer and A. Fasolino, Surface Science 605, (2011) 1611.
3. L. Wirtz, A. Rubio, Solid State Commun. 131 (2004) 141.
4. I.M. Lifshitz, Zh. Eksp. Teor. Fiz. 22 (1952) 475.
5. H. Yanagisawa, T. Tanaka, Y. Ishida, M. Matsue, E. Rokuta, S. Otani, C. Oshima, Surf. Interface Anal. 37 (2005) 133.
6. N. Mounet, N. Marzari, Phys. Rev. B 71 (2005) 205214.
7. B. Fultz, Progress in Materials Science, 5 (2010) 247.

## Detection and identification of impurity components by THz scattering

**Author:** Oleg Gerasymov<sup>1</sup>; Liudmyla Sidletska<sup>1</sup>

<sup>1</sup> Odesa Mechnikov National University

**Corresponding Author:** milapolonskaa@gmail.com

The results of THz radiation scattering experiments on granular composites are interpreted through a combined scenario of ballistic photon propagation and scattering. At low impurity concentrations, the refractive index varies linearly with concentration, indicating predominantly ballistic transport. As the impurity content increases, multiple scattering becomes more significant. However, near dense packing, scattering intensity decreases, suggesting a return to ballistic behavior within the impurity phase. The observed nonmonotonic scattering behavior serves as a marker for identifying impurity presence and properties, making THz spectroscopy an effective tool for applied diagnostics.

## Chosen topics in topological condensed matter

**Author:** Flavio Nogueira<sup>1</sup>

<sup>1</sup> *IFW Dresden*

**Corresponding Author:** f.de.souza.nogueira@ifw-dresden.de

We will give an introduction to the use of topology as a way to understand certain condensed matter systems. To this end we choose some topics of current interest to the research community. One basic example is given by formulating the quantum Hall conductivity as a manifestation of the Gauss-Bonnet theorem. A slightly more sophisticated example that we will discuss, is the axion electrodynamics of topological materials. We will explain how the axion electrodynamics differs from ordinary textbook-level electrodynamics. The simplest version of it, applied to topological insulators, just leads to a change in the boundary conditions of the Maxwell equations.

## Partition Function Zeros and Finite-Size Effects in the Blume–Capel Model on a Complete Graph

Yulian Honchar

**Author:** Yulian Honchar<sup>1</sup>

<sup>1</sup> *Yukhnovskii Institute for Condensed Matter Physics*

**Corresponding Author:** julkohon@icmp.lviv.ua

The Blume–Capel model, an extension of the Ising model with single-ion anisotropy, features a rich phase diagram with the first- and second-order phase transition lines intersecting at the tricritical point. While the exact solution is known in the thermodynamic limit for a complete graph, finite-size effects remain less understood. This talk presents an overview of recent results obtained by analyzing partition function zeros in complex temperature, magnetic field, and crystal field planes. These zeros offer complementary insights into the system's critical behavior and its finite-size scaling. The results show that effective criticality persists even in large systems, with partition function zeros revealing the gradual crossover to the asymptotic mean-field behavior. Distinctions between critical and tricritical behavior are particularly evident when comparing Fisher, Lee–Yang, and crystal-field zeros, making this approach a powerful tool for characterizing phase transitions in finite systems.

1. Yulian Honchar, Mariana Krasnytska, Bertrand Berche, Yuriy Holovatch, Ralph Kenna. Partition function zeros for the Blume-Capel model on a complete graph. *Low Temp. Phys.* vol. 51 (2025) pp. 634-645.

## Mathematical Physics

### Effective form factors for asymptotics of finite-temperature correlation functions

**Author:** Oleksandr Gamayun<sup>1</sup>

<sup>1</sup> *LIMS*



**Corresponding Author:** oleksandr.gamayun@gmail.com

The behavior of correlation functions in one-dimensional quantum systems at zero temperature is now very well understood in terms of linear and non-linear Luttinger models. The “microscopic” justification of these models consists in the exact accounting for soft-mode excitations around the vacuum state and, at most few high-energy excitations. At finite temperature, or more generically for finite entropy states, this direct approach is not applicable due to the different structure of “soft” excitations. We focus on physical systems where the strong interaction makes it possible to present correlation functions in terms of Fredholm determinants of the generalized sine kernels. Based on “microscopic” resummations, we develop a phenomenological approach of the effective form factors that allows us to describe the asymptotic behavior of these Fredholm determinants. We demonstrate how this works for correlation functions in the XY model, mobile impurity, and the generic Toeplitz determinants. We explain how this approach is related to the Riemann-Hilbert methods.

## Zeros of isomonodromic tau functions and holomorphic anomaly equation

**Author:** Pavlo Gavrylenko<sup>1</sup> Giulio Bonelli<sup>1</sup>; Ideal Majtara<sup>1</sup>; Alessandro Tanzini<sup>1</sup>

<sup>1</sup> SISSA, Trieste, Italy

**Corresponding Author:** pasha145@gmail.com

Isomonodromic tau functions have explicit expressions as sums of  $c=1$  conformal blocks (or Nekrasov functions), known as the Kyiv formulas, discovered by Gamayun, Iorgov, and Lisovyy. The zeros of these tau functions are described by classical, or  $c=\infty$  conformal blocks, also identified with the Painlevé action on the trajectory. We analyze an expansion of the tau function around its zero and combine it with the genus expansion of the conformal block. Modular properties of the tau function are well-defined and imply the modular properties of the conformal block. Namely, we prove that the conformal block satisfies the so-called holomorphic anomaly equation as a function of  $E_2$  quasimodular form. The talk will be based on the paper <https://arxiv.org/abs/2410.17868>.

## Integrable spinning fluid

**Author:** Andrii Liashyk<sup>1</sup>

<sup>1</sup> BIMSA

**Corresponding Author:** a.liashyk@gmail.com

The one-dimensional Calogero-Moser model is a well-established integrable model describing  $N$  interacting particles in both classical and quantum frameworks. In their seminal paper, Abanov, Bettelheim, and Wiegmann demonstrated that a collective description of this model gives rise to integrable hydrodynamics similar to the Benjamin-Ono system. These interacting particle systems can also be extended to include integrable spin generalizations, where internal degrees of freedom are assigned to each particle. In our paper we discuss the hydrodynamic formulation of the spin Calogero-Moser system, which emerges as an integrable spinning fluid system, and elucidate its connection to the matrix Benjamin-Ono equation recently introduced.

## Perturbative connection formulas for Heun equations

**Author:** Andrii Naidiuk<sup>1</sup>

<sup>1</sup> *University of Tours*

**Corresponding Author:** andnai@ukr.net

We recover the predictions of CFT regarding the connection formulae for the family of Heun equations. Two methods of derivation of the connection coefficients are employed: the theorem of Schäfer and Schmidt that allows for a rigorous proof in some cases, as well as the analysis of the asymptotic behavior of the Floquet solutions. Both methods yield closed formulas in terms of continued fractions which can be compared with the results obtained from CFT by means of Zamolodchikov conjecture. We will review two simple cases of the application of these methods: the reduced confluent Heun equation and the Mathieu equation

## Motion in perturbed Schwarzschild space-time

**Author:** Oleksii Yanchyshen<sup>1</sup>

<sup>1</sup> *Bogolyubov Institute for Theoretical Physics*

**Corresponding Author:** afdsrqwg@gmail.com

We obtain relativistic Gaussian perturbation equations for osculating elements in Schwarzschild space-time background, for an arbitrary force not restricted to the equatorial plane. As an application, we solve the perturbation equations in linear approximation for force induced by the Kerr space-time as an expansion of the Schwarzschild space-time. For this case in post-Newtonian limit, we reproduce known Lense-Thirring original results. Also, we consider motion in the  $q$ -metric space-time, which can be treated as the space-time of a BH with a quadrupole moment. For both space-times, we obtain relativistic observables.

## Defect fusion in higher dimensions

**Author:** Oleksandr Diatlyk<sup>1</sup>

<sup>1</sup> *New York University*

**Corresponding Author:** od2051@nyu.edu

In this talk, I will discuss defect conformal field theory (DCFT), with a focus on results from [1]. DCFT provides a powerful framework for studying quantum and statistical systems in the presence of localized objects, such as impurities, boundaries, or defects. These structures naturally arise across diverse areas of physics—from condensed matter to string theory—and can dramatically alter the behavior of the bulk system.

To illustrate this point, I will briefly review the Kondo effect, where a single magnetic impurity in a sea of conduction electrons leads to a nontrivial infrared (IR) fixed point and modifies the resistivity at low temperatures. This classic problem can be recast in terms of conformal boundary conditions, highlighting how impurities can drive strongly coupled physics even in otherwise free theories.

I will then discuss one result from [1], concerning the study of localized magnetic field lines in the critical  $O(N)$  model. Working in coordinates  $x = (y, z, x)$ , the defects are extended along the  $y$ -direction and are separated along the transverse  $z$ -direction by a distance  $r$ :

$$S = \int d^d x \left( \frac{1}{2} (\partial_\mu \varphi_I)^2 + \lambda_b \Lambda^{4-d} T^4 (\varphi_I \varphi_I)^2 \right) + h_{1,ba}^{\frac{d-4}{2}} D \int dy \hat{n} \cdot \varphi(y, z=0, x=0) + h_{2,ba}^{\frac{d-4}{2}} D \int dy \hat{m} \cdot \varphi(y, z=r, x=0). \quad (1)$$

We denote these defects as  $\mathcal{D}(\hat{n})$  where the unit vector  $\hat{n} \in S^{N-1}$  specifies the orientation of the defect in the  $O(N)$  directions. I will show that the fusion product among the defect lines labeled by  $\hat{n}, \hat{m} \in S^{N-1}$  takes the following intuitive form:

$$\mathcal{D}(\hat{n}) \circ \mathcal{D}(\hat{m}) = \mathcal{D}\left(\frac{\hat{n} + \hat{m}}{\sqrt{2(1 + \hat{n} \cdot \hat{m})}}\right). \quad (2)$$

I will also present the Casimir energy using the  $\epsilon$  expansion:

$$\mathcal{E}(\hat{n}, \hat{m}) = -(\hat{n} \cdot \hat{m}) \frac{N+8}{4\pi} - \epsilon \frac{1}{4\pi} \left[ \frac{(\hat{n} \cdot \hat{m}) N^2 - 3N - 22}{2(N+8)} - (1 + 2(\hat{n} \cdot \hat{m})^2) \frac{\pi^2(N+8)}{16} \right]. \quad (3)$$

These results provide an example of non-topological line defect fusion in an interacting CFT and may have further implications for understanding impurity-driven phase transitions in critical systems.

1. O. Diatlyk, H. Khanchandani, F. K. Popov, and Y. Wang, *JHEP* 09 (2024) 006, doi:10.1007/JHEP09(2024)006, arXiv:2404.05815 [hep-th].

## Isomonodromic tau function for Painleve I equation via irregular conformal blocks of rank 5/2

**Author:** [Yurii Zhuravlov](#)<sup>1</sup>; [Nikolai Iorgov](#)<sup>1</sup>; [Oleg Lisovyy](#)<sup>2</sup>; [Kohei Iwaki](#)<sup>3</sup>

<sup>1</sup> *Bogolyubov Institute for Theoretical Physics of the National Academy of Sciences of Ukraine*

<sup>2</sup> *Institut Denis-Poisson, Université de Tours*

<sup>3</sup> *The Graduate School of Mathematical Sciences, The University of Tokyo*

**Corresponding Author:** [ujpake@gmail.com](mailto:ujpake@gmail.com)

Recently, there were developed notion of irregular conformal blocks in two dimensional conformal field theory. It is believed that the conformal blocks are related to the isomonodromic tau functions of Painleve equations. I will review how it works on the concrete example of Painleve I equation. The main idea is that the isomonodromic tau function of Painleve I equation is presented in the form of Fourier series (Zak transform). Its main building block admits several conjectural interpretations, such as the partition function of an Argyres-Douglas gauge theory, the topological recursion partition function for the Weierstrass elliptic curve, and a 1-point conformal block on the Riemann sphere with an irregular insertion of rank 5/2. I will focus on the algebraic construction of the rank 5/2 Whittaker state for the Virasoro algebra.

## 1/2-BPS line defects in 4d N=2 SQFTs via Cohomological Hall algebras

**Author:** [Nikita Grygoryev](#)<sup>1</sup>; [Davide Gaiotto](#); [Wei Li](#)

<sup>1</sup> *Perimeter Institute / University of Waterloo*

**Corresponding Author:** grygoryevnikita1512@gmail.com

Supersymmetric quantum field theories (SQFTs), particularly those with  $N=2$  supersymmetry in four dimensions, often exhibit intricate behaviors. Yet, their rich structures can be more tractable than those of their non-supersymmetric counterparts. Notably, their BPS sectors are governed by algebraic frameworks reminiscent of those in simpler holomorphic-topological models.

In this talk, I will focus on the  $1/2$ -BPS line defects in such theories, which are expected to form monoidal categories endowed with additional structures, such as rigidity and a system of renormalized  $r$ -matrices. These structures encapsulate the fusion, duality and "meromorphic" braiding properties of lines.

Building upon this, we propose a construction that associates to each theory a category of bimodules over the Cohomological Hall Algebra (CoHA) derived from its BPS quiver. This category is designed to mirror the anticipated properties of the category of line defects, providing a bridge between the physical intuition and mathematical formalism.

Based on joint work with Davide Gaiotto and Wei Li.

## Statistical model of dimers and counting of boxes

**Author:** Mykola Semenyakin<sup>1</sup>

<sup>1</sup> *Perimeter Institute for Theoretical Physics*

**Corresponding Author:** semenyakinms@gmail.com

The statistical models of dimers belong to the class of so-called free fermionic exactly solvable models. This means, that every correlation function of local operators in this model can be computed by determinant of some matrix, and, moreover, can be expressed using only two-point functions, i.e. the Wick's contraction formula is satisfied. Many other models of statistical physics can be mapped onto certain models of dimers. In my talk I will explain how the counting of 3d Young diagrams (or boxes in the corner) can be mapped onto model of dimers, and how this boxcounting can be generalized in intriguing ways.

## Astrophysics and Cosmology

### Angular Power Spectrum of the 21 cm Signal from the Dark Ages: Sensitivity to Cosmological Parameters

**Author:** Danylo Koval<sup>1</sup>; Bohdan Novosyadlyj<sup>1</sup>

<sup>1</sup> *Astronomical Observatory of Ivan Franko National University of Lviv*

**Corresponding Author:** kiwisyn@gmail.com

The 21 cm line of neutral hydrogen provides a powerful observational window into the early Universe, particularly during the Dark Ages (redshifts  $z \sim 30 - 200$ ), before the emergence of the first luminous objects. In this work, presented a theoretical study of the angular power spectrum  $C_{\ell}$  of 21 cm brightness temperature fluctuations and its dependence on key cosmological parameters.

Described a linear perturbation framework that accounts for density inhomogeneities, peculiar velocities (redshift-space distortions). By modeling the 3D power spectrum of the 21 cm signal and projecting it into angular multipole space, could be investigated the sensitivity of  $(C_{\ell})$  to variations in parameters such as the total matter density  $(\Omega_m)$ , baryon fraction  $\Omega_b$ , Hubble constant  $H_0$ , and the fluctuation amplitude  $\sigma_8$ .

Results show that the 21 cm angular power spectrum is sensitive to these parameters, especially at high multipoles where small-scale information is preserved. This highlights the potential of future radio interferometric observations—such as those by the Square Kilometre Array (SKA)—to provide competitive constraints on the cosmological model.

*Acknowledgments.* This work is done in the framework of the project “Tomography of the Dark Ages and Cosmic Dawn in the lines of hydrogen and the first molecules as a test of cosmological models” (state registration number 0124U004029) supported by the National Research Foundation of Ukraine.

## Sensitivity of the redshifted 21 cm signal from Dark Ages to parameters of primordial magnetic fields

**Author:** Bohdan Novosyadlyj<sup>1</sup>; Nazarii Fortuna<sup>1</sup>; Yurii Kulinich<sup>1</sup>; Anton Rudakovskiy<sup>2</sup>

<sup>1</sup> Ivan Franko National University of Lviv

<sup>2</sup> Bogolyubov institute for theoretical physics]

**Corresponding Author:** fortunazar@gmail.com

We study the impact of primordial magnetic fields on the global 21 cm signal during the Dark Ages. By modeling magnetic heating effects, we show that the signal is sensitive to PMFs amplitude and spectral index, offering a potential probe of early-universe magnetogenesis with upcoming 21 cm observations.

*Acknowledgments.* This work is done in the framework of the project “Tomography of the Dark Ages and Cosmic Dawn in the lines of hydrogen and the first molecules as a test of cosmological models” (state registration number 0124U004029) supported by the National Research Foundation of Ukraine.

## Bayesian analysis of Starobinsky and Higgs inflation models with reheating in light of ACT and DESI data releases

**Author:** Dmytro Zharov<sup>1</sup>; Oleksandr Sobol<sup>1,2</sup>; Stanislav Vilchinskii<sup>1,3</sup>

<sup>1</sup> Taras Shevchenko National University of Kyiv

<sup>2</sup> Institute for Theoretical Physics, University of Münster

<sup>3</sup> Departement de Physique Theorique and Center for Astroparticle Physics,

**Corresponding Author:** dmitriy.zharov.02@knu.ua

In the recent sixth data release (DR6) of the Atacama Cosmology Telescope (ACT) collaboration, the value of  $n_s = 0.9743 \pm 0.0034$  for the scalar spectral index is reported, which excludes the Starobinsky and Higgs inflationary models at  $2\sigma$  level. In this paper, we perform a Bayesian inference of the parameters of the Starobinsky or Higgs inflationary model with non-instantaneous reheating using the Markov chain Monte Carlo method. For the analysis, we use observational data on the cosmic microwave background collected by the Planck and ACT collaborations and on baryonic acoustic oscillations from the Dark Energy Spectroscopic Instrument (DESI) collaboration. The reheating stage is modelled by a single parameter  $R_{\text{reh}}$ , which contains a combination of the reheating temperature

$T_{\text{reh}}$  and the effective equation of state of matter during reheating  $\bar{\omega}_{\text{reh}}$ . Using the modified Boltzmann code CLASS and the cobaya software with the GetDist package, we perform a direct inference of the model parameter space and obtain their posterior distributions. Using the Kullback–Leibler divergence, we estimate the information gain obtained from the observed data: In the proposed parameterization, we get 8.66 bits of information about the amplitude of the inflaton potential and 2.52 bits of information about the reheating parameter.

Inclusion of the ACT DR6 data provides 75% more information about the reheating stage compared to analysis without ACT data. In addition, we draw constraints on the reheating temperature and the average equation of state. While the former can vary within 10 orders of magnitude, values in the 95% credible interval indicate a sufficiently low reheating temperature; for the latter there is a clear preference for values greater than 0.5, which means that the conventional equations of state for dust  $\omega = 0$  and relativistic matter  $\omega = 1/3$  are excluded with more than  $2\sigma$  level of significance. Nevertheless, there still is a big part of parameter space where Starobinsky and Higgs inflationary models exhibit a high degree of consistency with the latest observational data, particularly from ACT DR6. Therefore, it is premature to reject these models.

## An Axion Pulsarscope

**Authors:** Mariia Khelashvili<sup>1</sup>; Mariangela Lisanti<sup>None</sup>; Anirudh Prabhu<sup>None</sup>; Benjamin Safdi<sup>None</sup>

<sup>1</sup> SISSA

**Corresponding Author:** mkhelash@sissa.it

Electromagnetic fields of pulsars can generate coherent axion signals at their rotational frequencies, which may be detected by laboratory experiments—pulsarscopes. As a promising case study, we model axion emission from the well-studied Crab pulsar, predicting a signal at  $f \approx 29.6$  Hz that would be present regardless of whether axions contribute to the dark matter abundance. We evaluate the sensitivity of upcoming axion dark matter detection experiments, such as DMRadio-GUT, Dark SRF, and CASPER, to this pulsar-sourced axion signal, using different magnetosphere models to capture uncertainties in astrophysical modeling. For instance, the Dark SRF experiment could probe axions with any mass below  $10^{-13}$  eV down to  $g_{a\gamma\gamma} \sim 3 \times 10^{-13} \text{ GeV}^{-1}$  with one year of data, assuming the vacuum magnetosphere model. This sensitivity may be lower depending on the degree to which the magnetosphere is screened by plasma. The potential of pulsar-sourced axions as a well-defined target for direct detection experiments motivates dedicated simulations of axion production in pulsar magnetospheres.

## Dynamical Friction for Plummer Sphere in Ultralight Dark Matter

**Author:** Andrii Zaporozhchenko<sup>1</sup>; Volodymyr Gorkavenko<sup>1</sup>; Eduard Gorbar<sup>1,2</sup>

<sup>1</sup> Taras Shevchenko National University of Kyiv

<sup>2</sup> Bogolyubov Institute for Theoretical Physics

**Corresponding Author:** zaporozhchenko.andrey@gmail.com

Among popular candidates for dark matter (DM) particles are weakly interacting massive particles (WIMPs) with masses of the order of 100 GeV, sterile right-handed neutrinos with masses of several keV, and axion-like particles with masses of  $\mu\text{eV}$ . We consider a model of ultralight dark matter (ULDM) because of its interesting phenomenology. ULDM is composed of bosonic particles with masses from  $10^{-23}$  to  $10^{-21}$  eV, and is hypothesized to form a Bose-Einstein condensate (BEC) on galactic scales. ULDM models could successfully reproduce the large-scale structure of the Universe

and are free of some problems which cold dark matter (CDM) models encounter at galactic scales, due to a very large de Broglie wavelength of order kpc.

In the present work, we studied the ground and vortex states of ULDM. We derived an expression for the dynamical friction force for objects of finite size modelled as a Plummer sphere. We also calculated radial and tangential components of the dynamical friction force acting on Plummer spheres traveling in a ULDM medium. Our findings reveal that the frictional force experienced by a Plummer sphere deviates from that of a point mass, particularly when the ratio of the sphere's radius to its orbital radius is more than  $10^{-2}$ . The finite size of a globular cluster introduces a friction correction of up to 10%.

Our study is relevant to the orbital decay of globular clusters moving through the dark matter halos of galaxies. According to standard gravitational theory, some clusters should have experienced significant dynamical friction in CDM, causing them to spiral inward and merge with the galactic center well within the age of the Universe. However, observations show that they remain at relatively large distances from the center. We plan to consider the ULDM model to address the globular cluster timing problem in the future.

1. V.M. Gorkavenko, A.I. Yakimenko, A.O. Zaporozhchenko, E.V. Gorbar, e-Print: 2412.15428 [astro-ph.GA] (2024)
2. V.M. Gorkavenko, A.O. Zaporozhchenko, E.V. Gorbar et al., e-Print: 2504.06448 [astro-ph.GA] (2025)

## Hydrodynamical Modeling of Stellar Wind Bubbles for Improved Photoionization Analysis

**Author:** [Andrii Pozdieiev](#)<sup>1</sup>; Bohdan Melekh<sup>1</sup>

<sup>1</sup> *Ivan Franko National University of Lviv*

**Corresponding Author:** andrii.pozdieiev@lnu.edu.ua

We present the first steps of a new approach aimed at improving photoionization analysis in dwarf galaxies by replacing unresolved features in chemodynamical simulations (Recchi and Hensler 2013) with physically consistent structures from hydrodynamical modeling. In previous works (Melekh et al. 2015, 2024), artificial thin dense shells (TDS) were introduced to emulate shock fronts that could not be resolved in chemodynamical simulations. To overcome this limitation, we initiated a transition to hydrodynamical simulations using the PLUTO code (Mignone et al. 2007), beginning with a 1D spherically symmetric model of a stellar wind from a single massive star. This setup reproduces the classical structure of a wind-blown bubble as described by Castor, McCray, and Weaver (1975, 1977), including the central hot shocked wind, the contact discontinuity, and the dense swept-up shell. Our results confirm the formation of these regions, including the TDS, and allow direct comparison with theoretical models of bubble evolution, validating the numerical approach. This structure serves as a foundation for subsequent photoionization modeling. The ultimate goal is to incorporate these hydrodynamic profiles into multi-component photoionization simulations to achieve more self-consistent results. This work sets the stage for extending the method to multi-dimensional simulations and full galaxy-scale outflows.

*Acknowledgments.* This work is done in the framework of the project "Tomography of the Dark Ages and Cosmic Dawn in the lines of hydrogen and the first molecules as a test of cosmological models" (state registration number 0124U004029) supported by the National Research Foundation of Ukraine.

## Detailed Photoionization Analysis of Chemodynamical Simulation Results for the Evolution of Dwarf Star-Forming Galaxies at an Age of 100 Myr

**Authors:** Mykhailo Shevchenko<sup>1</sup>; Bohdan Melekh<sup>1</sup>

<sup>1</sup> *Ivan Franko National University of Lviv*

**Corresponding Author:** mykhailo.shevchenko@lnu.edu.ua

During the modification of multicomponent photoionization models (MPhM) of nebular emission surrounding regions of active star formation, developed to analyze chemodynamical simulations of the evolution of a dwarf galaxy characterized by intense star-forming activity (which account for the age-dependent variations in chemical abundances, gas density, and temperature within the "superwind" region), a significant problem arises related to the treatment of the diffuse ionizing radiation (DIR) field within the nebular environment. Typically, the *Outward-only* approximation is employed for this purpose [1, 2]. However, the inhomogeneous ionization structure of the nebular medium, as revealed by chemodynamical simulations of these objects, suggests that the presence of an ionization front in the equatorial sectors of the dwarf galaxy may be a numerical artifact caused by incorrect DIR calculation. In [3], a procedure for the detailed calculation of DIR within the framework of multicomponent photoionization modeling was proposed. The authors applied this method to an MPhM corresponding to an evolutionary age of 140 Myr. As expected, the resulting ionization structure in the equatorial sectors differs substantially from the one obtained using the *Outward-only* approximation.

In the present work, we compare the results of MPhM for an evolutionary age of 100 million years. The initial spatial maps of emissivity and opacity (MEO) for a wide range of photon energies (both continuum and line emission) were obtained using the *Outward-only* approximation with the Cloudy code [4]. These maps were subsequently used for a detailed calculation of the DIR field using the DiffRay code [3]. The updated MEOs were then employed to recalculate the MPhM using the Cloudy code, taking into account the DIR field precomputed by DiffRay. As a result, the obtained ionization structure differs significantly from the initial one (derived under the *Outward-only* approximation) underscoring the necessity of further Cloudy + DiffRay iteration cycles. Here we present the resulting ionization structure obtained after the second global iteration.

*Acknowledgments.* This work is done in the framework of the project "Tomography of the Dark Ages and Cosmic Dawn in the lines of hydrogen and the first molecules as a test of cosmological models" (state registration number 0124U004029) supported by the National Research Foundation of Ukraine.

1. B. Melekh, S. Recchi, G. Hensler and O. Buhajenko, Photoionization analysis of chemodynamical dwarf galaxies simulations, MNRAS 450, 111–127 (2015).
2. B. Melekh, S. Recchi, G. Hensler and O. Buhajenko, Erratum: Photoionization analysis of chemodynamical dwarf galaxies simulation, MNRAS 502, 1048–1050 (2021).
3. B. Melekh, O. Buhajenko, I. Koshmak, Photoionization analysis of chemodynamical dwarf galaxies simulations. II. Detailed calculation of diffuse ionizing radiation, MNRAS 532, 524–537 (2024).
4. G. Ferland, Hazy, A Brief Introduction to Cloudy\*, Version 08 (University of Kentucky Internal Report, 2008), 807 p.

## Multicomponent Photoionization Modelling of the First Dwarf Galaxies

**Authors:** Serhii Chudyk<sup>1</sup>; Bohdan Melekh<sup>1</sup>; Ihor Koshmak<sup>1</sup>

<sup>1</sup> *Ivan Franko National University of Lviv*

**Corresponding Author:** chyduksergiy321@gmail.com

The epoch of cosmic reionization marks a pivotal stage in the history of the Universe, during which the first sources of ionizing radiation transformed the intergalactic medium from a neutral to an ionized state. While it was traditionally believed that massive galaxies and quasars played the dominant role in this process, recent observations and theoretical models increasingly suggest that low-luminosity dwarf galaxies may have been key contributors to early Universe reionization due to their large number and radiation efficiency [1, 2]. Thus, studying the spectral properties of ionizing radiation emitted by dwarf galaxies is crucial for understanding the early cosmological evolution of the Universe, as it provides critical insights into their contribution to the ionizing photon budget and the nature of early galaxy populations.



Accurately modeling spectral energy distribution (SED) of dwarf galaxies requires detailed consideration of the hydrodynamic structure of their nebular environment, since ionizing radiation from stars passes through the nebular environment surrounding the star-forming region before reaching the intergalactic medium. The morphology of the nebula is shaped by a superwind originating from the central region, which hosts young, extremely low-metallicity stars.

This work proposes a new analytical–numerical method for the multicomponent photoionization modelling, developed on the basis of the approach presented by Koshmak and Melekh (2018) [3], which enables the reproduction of the main hydrodynamic characteristics of a superwind bubble structure observed in high-resolution hydrodynamic simulations, while requiring minimal computational resources. The proposed approach not only reproduces the evolution of the superwind bubble, but also allows for detailed consideration of all important elementary processes that provide the ionizing radiation transfer through the inhomogeneous nebular environment. A key advantage of our model is the ability to track the transformation of the ionizing spectral energy distribution as it propagates through the distinct nebular components of a superwind bubble.

We compute the ionization structure and spectrum of ionizing radiation passing through the components of the nebular environment of a dwarf galaxy surrounding the region of active star formation during the era of cosmic reionization of the Universe. The resulting models provide SEDs of output radiation from dwarf galaxies into the intergalactic medium. After such radiative transfer, output SED contains the emission lines, with the Ly $\alpha$  line in particular showing strong intensity, which may significantly affect the spectra of the first molecules.

*Acknowledgments.* This work is done in the framework of the project “*Tomography of the Dark Ages and Cosmic Dawn in the lines of hydrogen and the first molecules as a test of cosmological models*” (state registration number 0124U004029) supported by the National Research Foundation of Ukraine.

1. H. Atek, I. Labbé, L. J. Furtak et al., Most of the photons that reionized the Universe came from dwarf galaxies, *Nature* 626, 975–978 (2024).
2. Z. Wu and A. Kravtsov, On the contribution of dwarf galaxies to reionization of the Universe, *Open Journal of Astrophysics* 7 (2024).
3. I. O. Koshmak and B. Ya. Melekh, The primordial helium abundance determination using multicomponent photoionization modelling of low-metallicity H II regions, *Advances in Astronomy and Space Physics* 8, 16–23 (2018).

## Photoionization analysis of chemodynamical simulations: Cloudy C23.01 vs C08.00

**Author:** Volodymyr Buhlak<sup>1</sup>; Bohdan Melekh<sup>1</sup>

<sup>1</sup> Ivan Franko National University of Lviv

**Corresponding Author:** volodymyr.buhlak@lnu.edu.ua

Photoionization modelling allows us to monitor the radiation transfer taking into account all important processes in nebular plasmas.

The spatial distributions of densities, chemical abundances and temperatures are needed for such modelling were obtained from chemodynamical simulations of dwarf galaxies. In present work we check the reliability of older version of CLOUDY C08.00 [1] in comparison with newest version - C23.01. The reason of this was small coding mistake since 90's fixed recently in CLOUDY C23.01 [2] which changed high-ionized gas clouds spectrum and also higher spatial resolution of newest version made us make sure that C08.00 is still reliable for final calculations. The our wrapper for multicomponent photoionization modelling (MPhM) [3, 4] based on chemodynamical simulations [5] was rewritten for C23.01 version. Then we recalculated one of MPhM using new MPhM wrapper based on C23.01 and compared the obtained ionization structure (the electron temperatures and densities, the radial distribution of recombination and forbidden lines emissivity and ionic oxygen abundances in various ionization stages) with one calculated earlier using old wrapper version based

on C08.00. Also we analyze the differences in these parameters as well as in predicted emission line spectra.

*Acknowledgments.* This work is done in the framework of the project "Tomography of the Dark Ages and Cosmic Dawn in the lines of hydrogen and the first molecules as a test of cosmological models" (state registration number 0124U004029) supported by the National Research Foundation of Ukraine.

1. Ferland G. J., 2008, *Hazy, a Brief Introduction to Cloudy, Version 08* (University of Kentucky Internal Report), p. 807, <http://www.nublado.org>
2. Gunasekera Ch. M., van Hoof P. A. M., Chatzikos M., Ferland G. J., The 23.01 Release of Cloudy, Research Notes of the AAS 7, 11, id.246 (2023).
3. Melekh B., Recchi S., Hensler G., Buhajenko O., 2015, MNRAS, 450, 111.
4. Melekh B., Buhajenko O., Koshmak I., 2024, MNRAS, 532.
5. Recchi S., Hensler G., 2013, A&A, 551, A41 (RH13).

## Artificial Intelligence in Physics

### The interaction between physics and machine learning: attractive or repulsive?

**Author:** Tymofii Nikolaienko<sup>1</sup>

<sup>1</sup> Taras Shevchenko National University of Kyiv

**Corresponding Author:** tim.n@knu.ua

The recent surge in machine learning (ML) capabilities, most widely known through the ascent of large language models, mirrors the transformative impact of microprocessors in the 1970s, indicating a potential paradigm shift in the computational toolset used in scientific research workflows, including physics. This talk aims to ignite interest in investigating the multifaceted relationship between physics and ML, mentioning both their "attractive" synergies and "repulsive" challenges. The nature of neural networks (NNs) makes them powerful, universal function approximators that are capable of solving the supervised learning problem, yet they suffer from a lack of interpretability which is critical for precise sciences. At the same time, there are striking parallels between the high-dimensional optimization landscapes of NN training and concepts from statistical physics, including phenomena akin to phase transitions, suggesting immense potential for physicists to contribute to the ML field. The field known today as physics-informed machine learning seeks to bridge these gaps by, for example, embedding physical symmetries directly into NN architectures, or by leveraging NNs as the solvers for the differential equations that underpin our physics-based simulation models. This talk will explore some of these avenues, aiming to ensure that the interaction between physics and machine learning can ultimately evolve into a 'stable, bound state' - a truly 'attractive' proposition for both disciplines.

### A neural network model of the dependence of the energy of biomolecules on structure and quantum-mechanical descriptors

**Authors:** Andrii Terets<sup>1</sup>; Tymofii Nikolaienko<sup>1</sup>

<sup>1</sup> Faculty of Physics of Taras Shevchenko National University of Kyiv

**Corresponding Author:** terets.andrey@gmail.com

The development of new molecules and the optimization of chemical synthesis depend on the ability to accurately estimate molecular energies and properties from structural information. In recent years, machine learning (ML) methods have emerged as powerful tools for addressing this task [1]. However, a persistent challenge is the illusion of improved accuracy that arises due to error compensation effects. This issue occurs when a ML model attempts to approximate the total energy directly, rather than modeling its individual physical components separately. By directly approximating the total energy, such models may rely on error compensation between components, which masks inaccuracies and undermines generalization to new molecular systems.

To address these challenges, we leverage principles from density functional theory (DFT) and graph neural networks (GNNs). Our approach aims to explore the feasibility of constructing a neural network model for predicting total molecular energy through a two-stage process. In the first stage, physically motivated descriptors are generated based on electron density and kinetic energy contributions, which are associated with individual atoms or atom pairs rather than the molecule as a whole. In the second stage, these descriptors are used to approximate the parameters of a classical interatomic potential using a separate neural network.

We demonstrate the effectiveness of our approach on publicly available datasets by accurately predicting both the total molecular energy and the electronic kinetic energy, with a mean absolute error (MAE) of 2.2 kcal/mol and 6.1 kcal/mol, respectively. Additionally, the model yields reliable results in the task of estimating intermolecular interaction energies, achieving a mean squared error (MSE) of 1.7 kcal/mol.

1. Sajjan M., Li J., Selvarajan R., Sureshbabu S.H., Kale S.S., Gupta R., Singh V., Kais S. Quantum machine learning for chemistry and physics // Chem. Soc. Rev. – 2022. – 51(15). – P. 6475–6573. – DOI: 10.1039/D2CS00203E.

## Galaxy Morphological Classification with Manifold Learning

**Authors:** Maksym Tsizh<sup>1</sup>; Vitalii Tymchyshyn<sup>2</sup>; Volodymyr Bezgubaa<sup>3</sup>; Vasyl Semenov<sup>3</sup>

<sup>1</sup> University of Bologna

<sup>2</sup> Bogolubov Institute for Theoretical Physics

<sup>3</sup> Kyiv Academic University

**Corresponding Author:** maksym.tsizh@lnu.edu.ua

We investigated classical machine learning algorithms for categorizing galaxy morphology using the Galaxy Zoo DECaLS dataset. It contains more than 300,000 photos of galaxies, from which we selected 50,000 images with the highest coincidence of human classification choice. Our methodology combined dimensionality reduction with subsequent classification. We evaluated five reduction techniques (LLE, Isomap, UMAP, t-SNE, PCA) followed by standard classifiers. Results show that preprocessing with Locally Linear Embedding (LLE) typically yielded the best performance for most classifiers, reaching accuracy levels comparable to basic neural networks. A key finding is that the 3D representation derived from LLE for shape analysis retained interpretability of reduced dimensions, a common challenge with nonlinear transformations. Additionally, applying k-means clustering in post-reduction data showed ambiguous results regarding natural data groupings; although one metric (Davies-Bouldin index) suggested four clusters aligning with astronomical human intuition, others (silhouette and elbow method, Dunn index) failed to identify a distinct structure.

## Accelerating Relativistic Heavy-Ion Collision Modeling: Machine Learning Integration with the iHKM Framework

**Authors:** Vladyslav Naboka<sup>1</sup>; Musfer Adzhymambetov<sup>1</sup>

<sup>1</sup> *Bogolyubov Institute for Theoretical Physics*

**Corresponding Author:** nvlad1@ukr.net

The integrated HydroKinetic Model (iHKM) is a key tool for simulating the complex dynamics of relativistic heavy-ion collisions. However, full-scale iHKM simulations are computationally demanding. This work presents a novel approach combining machine learning with iHKM to both infer optimal model parameters (such as viscosity and relaxation time) from experimental data and to approximate full simulation results with high speed and accuracy. The synergy of physics-based modeling and AI significantly accelerates the analysis pipeline, offering new possibilities for exploring collision energy regimes. The methodology and its validation on experimental datasets will be discussed.

## Implementation of a methodology for crystal structure prediction using genetic algorithms integrated into the Python ASE library

**Authors:** Bohdan Semeniuk<sup>1</sup>; Oleh Feia<sup>1</sup>

<sup>1</sup> *Kyiv Academic University*

**Corresponding Author:** semenuk.b.20@gmail.com

This talk is dedicated to the development and implementation of a methodology for crystal structure prediction using genetic algorithms integrated into the Python ASE library. The application of genetic algorithms for crystal structure prediction holds great potential in various fields, particularly in materials science and nanotechnology. The main objective is to develop an efficient tool that enables automation and acceleration of the process of finding optimal crystal structures for specific applications.

## Predicting superconductors critical temperature via machine learning methods

**Authors:** Ihor Svyarskyi<sup>1</sup>; Volodymyr Bezguba<sup>1</sup>

<sup>1</sup> *Kyiv Academic University*

**Corresponding Author:** i.svyarskyi@kau.edu.ua

The intriguing phenomenon of superconductivity has been extensively studied for over a century. Yet, a key challenge remains unresolved in practice: understanding and predicting the critical temperature  $T_c$  of a superconductor. This issue is especially challenging for high-temperature superconductors (HTSC), which comprise diverse material classes and probably involve different electron pairing mechanisms.

In this work, we apply machine learning to address this challenge using the 3DSC dataset [1], with  $T_c$  values sourced from the SuperCon database [2]. The dataset integrates several descriptor types: the DSOAP representation – a modified Smooth Overlap of Atomic Positions (SOAP) framework that enables modeling of doped and non-stoichiometric compounds, which are especially common among HTSCs; basic atomic attributes from the MAGPIE descriptor set [3]; and materials properties computed via DFT from the Materials Project (MP) [4].

We explore dimensionality reduction via Principal Component Analysis (PCA), unsupervised clustering of superconductors, and optimization of three regression models – K-nearest neighbors, Random Forest, and Gradient Boosting – to predict  $T_c$ . Despite the limited data (less than 4000 compounds,

including around 900 HTSCs), our models achieve competitive  $R^2$  values, with the best scores exceeding 0.89.

A novel aspect of our approach is the integration of electronic structure information. We introduce features based on the electronic density of states (DOS), derived from a reworked DOS fingerprint [5], as well as a simple descriptor counting the number of bands crossing the Fermi level. Both sets of features are obtained from the MP. The inclusion of DOS-based features and information about band-crossing provide a richer representation of electronic structure, which is often overlooked. This integrated approach has the potential to support large-scale screening of DFT-computed materials databases, helping to identify promising candidates for new superconductors.

## References

1. T. Sommer, R. Willa, J. Schmalian, and P. Friederich, "3DSC – a dataset of superconductors including crystal structures," *Scientific Data* 10(1), (2023), doi:10.1038/s41597-023-02721-y.
2. V. Stanev et al., "Machine learning modeling of superconducting critical temperature," *npj Computational Materials* 4(1), (2018), doi:10.1038/s41524-018-0085-8.
3. L. Ward, A. Agrawal, A. Choudhary, and C. Wolverton, "A general-purpose machine learning framework for predicting properties of inorganic materials," *npj Computational Materials* 2(1), (2016), doi:10.1038/npjcompumats.2016.28.
4. A. Jain et al., "Commentary: The Materials Project: A materials genome approach to accelerating materials innovation," *APL Materials* 1(1), (2013), doi:10.1063/1.4812323.
5. M. Kuban, S. Rigamonti, M. Scheidgen, and C. Draxl, "Density-of-states similarity descriptor for unsupervised learning from materials data," *Scientific Data* 9(1), (2022), doi:10.1038/s41597-022-01754-z.

## Broadband single-layer dielectric anti-reflective solar cell coatings

**Author:** [Anton Ovcharenko](#)<sup>1</sup>; Oleh Yermakov<sup>1,2</sup>

<sup>1</sup> V. N. Karazin Kharkiv National University

<sup>2</sup> Leibniz Institute of Photonic Technology, Jena, Germany

**Corresponding Author:** antathome23@gmail.com

A third to a half of solar radiation is reflected from a silicon surface of a bare solar cell. That is why a problem of creation additional anti-reflective coatings gathers lots of attention even today. In our submission, we demonstrate that a single patterned polycrystalline silicon layer can suppress average reflectance to  $\approx 2\%$  at normal incidence and below 5 % up to  $60^\circ$  across the 500–1200 nm band—performance that rivals state-of-the-art multilayer dielectric stacks while remaining fully CMOS-compatible. We describe two complementary strategies. First, a forward parametric sweep explores hybrid cross-circle meta-atoms, optimizing five geometric parameters with rigorous coupled-wave analysis (RCWA). Second, an inverse free-form route employs a ResNet-based generative latent optimization network (GLOnet) accelerated by adjoint RCWA, allowing the optimizer to discover manufacturable binary patterns on a 380 nm lattice in only a few hours on a modest CPU cluster.

Both routes independently converge on Huygens-type unit cells that satisfy a generalized Kerker condition, forwarding light efficiently into silicon with negligible absorption. The best cross-circle design already reduces weighted reflectance to 5 %, but the machine-learning-derived free-form geometry pushes it down to 4.4 % while retaining a manufacturable design.

Our results reveal that rapid forward sweeps give valuable physical intuition, while AI-assisted inverse design locates near-global optima that human intuition alone might miss, all within a single-layer process window. The demonstrated combination of ultrabroadband performance, wide angular

acceptance, polarization insensitivity and single-step fabrication positions such silicon metasurfaces as practical antireflection solutions for next-generation solar cells, photodetectors and integrated photonic systems.